

Estimation of a non-stationary model for annual precipitation in southern Norway using replicates of the spatial field

Rikke Ingebrigtsen^{*1}, Finn Lindgren², Ingelin Steinsland¹ and Sara Martino³

¹*Department of Mathematical Sciences, Norwegian University of Science and Technology (NTNU), Trondheim, N-7491, Norway*

²*Department of Mathematical Sciences, University of Bath, Claverton Down, Bath, BA2 7AY, United Kingdom*

³*SINTEF Energy Research, Trondheim, N-7491, Norway*

Abstract

Estimation of stationary dependence structure parameters using only a single realisation of the spatial process, typically leads to inaccurate estimates and poorly identified parameters. A common way to handle this is to fix some of the parameters, or within the Bayesian framework, impose prior knowledge. In many applied settings, stationary models are not flexible enough to model the process of interest, thus non-stationary spatial models are used. However, more flexible models usually means more parameters, and the identifiability problem becomes even more challenging. We investigate aspects of estimation of a Bayesian non-stationary spatial model for annual precipitation using observations from multiple years. The model contains replicates of the spatial field, which increases precision of the estimates and makes them less prior sensitive. Using `R-INLA`, we analyse precipitation data from southern Norway, and investigate statistical properties of the replicate model in a simulation study. The non-stationary spatial model we explore belongs to a recently introduced class of stochastic partial differential equation (SPDE) based spatial models. This model class allows for non-stationary models with explanatory variables in the dependence structure. We derive conditions to facilitate prior specification for these types of non-stationary spatial models.

Keywords: Non-stationary spatial modelling; Gaussian random fields; Gaussian Markov random fields; Stochastic partial differential equations; Annual precipitation; Bayesian inference

^{*}Corresponding author

1 Introduction

At the core of any statistical analysis is the wish to learn about a process or phenomena based on available data. The purpose of the analysis can be to gain insight about the process of interest and/or make predictions related to this process. In this paper, we study annual precipitation in southern Norway, and we aim both to learn about this process from data, and make predictions at spatial locations without observations.

To be able to learn about a process from data we need a model that is 1) realistic, 2) interpretable, and 3) possible to draw inference from with the available data. For most realistic processes, compromises between these three aims are necessary. We can simplify the model, impose more knowledge or restrictions, or get more data. In this paper, we use a model that is based on physical understanding, but is very simplified. A Bayesian approach is taken, and knowledge about the system is expressed through carefully chosen prior distributions. Further, we are able to utilise more data to learn about the precipitation process by extending the model such that several years of annual precipitation observations can be used.

The precipitation process is driven by humidity, changes in circulations, weather patterns and temperature, as well as interactions with the topography. Southern Norway is separated by the mountain range Langfjella: to the west there is a mountainous coastline dominated by large fjords, while eastern Norway has a more gentle landscape consisting of valleys and lowlands. This topographical difference is reflected in the climate. Humid oceanic winds hit the west coast and are forced to ascend due to the mountains. The result is that the western part of Norway receives high amounts of precipitation, while the eastern part is relatively dry being located in the “rain shadow”. This phenomenon is known as orographic precipitation. Statistical modelling and spatial prediction of precipitation in Norway are challenging tasks ([Orskaug et al., 2011](#); [Ingebrigtsen et al., 2014](#); [Dyrddal et al., 2014](#)). In some areas there are large variations in the amount of precipitation within relatively short distances, while other areas are more homogeneous. These features can be explained by the physics of the precipitation process in a complex and diverse terrain.

The main purpose of precipitation interpolation in Norway is as input to hydrological forecasting models to predict run-off either for flood warnings or to better schedule hydro-power production. Because of the topography, most of the catchment (where prediction is of interest) is often in mountainous areas, while the precipitation gauges (observations) are located in lower areas due to easier and cheaper maintenance. It is not uncommon that all the closest precipitation gauges are at lower elevation than the lowest point of the catchment of interest. Since changes in elevation is one of the driving forces of precipitation, this causes a problem of non-preferential sampling, and to do spatial interpolation we will need to do extrapolation with respect to elevation. This calls for a model with a physical basis, and a way to tackle this challenge is to include elevation in the model.

A statistical model for annual precipitation over southern Norway should have

two important properties. We have already argued that elevation should be included in the model. In addition, as locations close in space are more alike than locations further apart, the model should also include a spatial process. If the dependence structure of a spatial process changes within the domain it is defined, the process is non-stationary. Because of the complex Norwegian topography, it is reasonable to use a non-stationary spatial process, and that the non-stationarity depends on the topography.

A flexible and popular framework for statistical modelling is hierarchical models. The general scheme consists of two levels. The first level is the likelihood part, which specifies the model for the observations given a latent field. The second level specifies the model for the latent field, which can consist of several terms, e.g. a term for elevation and a spatial process. Both levels of the hierarchy contain parameters we would like to infer something about based on the observations. With a likelihood approach to inference, identifiability (or estimability) might become an issue. It is not always possible to estimate all parameters, but rather only some of them, or a function of them. Furthermore, one often does not know whether there are identifiability issues (Lele et al., 2010).

A Bayesian approach is often taken within the hierarchical modelling framework. In the Bayesian paradigm the identifiability challenge is solved by introducing a third level in the hierarchy; prior models for the parameters. Prior specifications for hierarchical model parameters are challenging for applied Bayesians, and common priors might have undesired properties (Gelman, 2006; Sørbye and Rue, 2014; Simpson et al., 2014). Especially if one is not aware of the identification properties, priors can give unintended inference consequences.

Gaussian random fields (GRFs) play an important role in spatial statistics; they are commonly used to model the spatial process itself, or as building blocks in hierarchical models (see e.g. Banerjee et al., 2004; Cressie and Wikle, 2011). The GRF is characterised by a mean function and a covariance function. In this paper, we use the stochastic partial differential equation (SPDE) approach introduced in Lindgren et al. (2011), where it was shown that Gaussian Markov random field (GMRF) approximations to GRFs with the Matérn covariance function can be derived from an SPDE formulation. The Markovian approximation enables fast simulations and inference, and integrated nested Laplace approximations (INLA, Rue et al., 2009) can be applied.

A constant mean GRF is stationary if the covariance function is invariant to spatial shifts. For many spatial processes a stationarity assumption is unrealistic, and there has been great interest in the literature to develop non-stationary spatial models, included contributions towards having explanatory variables in the dependence structure. Deformation methods obtain a non-stationary model by deformation of a latent space where the process is stationary (Sampson and Guttorp, 1992), and the axes of this latent space can be defined by explanatory variables (Schmidt et al., 2011). Another approach is spatial convolution models, where smoothing kernels are convolved with a white noise process (Higdon et al., 1999; Paciorek and Schervish, 2006), or with a spatial dependent process (Fuentes, 2002), to obtain

non-stationarity. [Reich et al. \(2011\)](#) extends the convolution model from [Fuentes \(2002\)](#) and use spatial covariates as kernels, while [Neto et al. \(2014\)](#) extends the convolution approaches in [Higdon et al. \(1999\)](#) and [Paciorek and Schervish \(2006\)](#) to incorporate covariates in the covariance structure. The SPDE formulation of [Lindgren et al. \(2011\)](#) also provides ways to easily introduce non-stationarity by letting the parameters or operators vary in space ([Lindgren et al., 2011](#); [Bolin and Lindgren, 2011](#); [Fuglstad et al., 2014b,a](#); [Ingebrigtsen et al., 2014](#)). We will use the approach in [Ingebrigtsen et al. \(2014\)](#), where the SPDE formulation is used, and non-stationarity is obtained by covariance parameters that depends on spatial explanatory variables.

A spatial model with an unknown spatially varying mean and a general non-stationary covariance is completely unidentifiable from one realisation of the process. Consider two models, where 1) the observations are exact observations of the spatially varying mean, and 2) the observations come from a model with a constant mean and a spatial field with a complex non-stationary dependence structure. The difference between these two models first appears when there are observed several replicates of the process. For model 1) the observations will for a given location be identical for all replicates. For model 2) the observations will vary between replicates according to the covariance model. Hence, the estimated model from one realisation is completely determined by the precise model choice and priors. Further, for spatial Gaussian models with known mean and a stationary Matérn covariance function, it has been shown that for a fixed domain and in-fill asymptotics there are no consistent estimators for all covariance parameters ([Zhang, 2004](#); [Kaufman and Shaby, 2013](#)), i.e. the variance of the estimators do not converge to zero as the number of observations increases. This means that even for a stationary model with known mean, there is limited information about some of the dependence parameters over a fixed domain from one realisation of the process. Therefore, spatial models, including specification of priors, have to be carefully chosen. Further, whenever possible, replicates of the process should be used to make inference. From a practical perspective, it is also easier to observe replicates of the spatial process, than it is to establish new sampling locations.

This paper is motivated by [Ingebrigtsen et al. \(2014\)](#), and the challenges reported there. [Ingebrigtsen et al. \(2014\)](#) suggest to use a Bayesian non-stationary SPDE based spatial model for annual total precipitation in southern Norway. The model has interpretable parameters, and the non-stationary model is shown to be superior to the corresponding stationary model with respect to the deviance information criterion (DIC, [Spiegelhalter et al., 2002](#)) and predictive performance. However, numerical problems and uncomfortable large prior sensitivity were reported. In a simulation study, some of the posterior mean estimates and credible intervals showed poor statistical properties, i.e. bias and low coverage. The model was interpretable and realistic, but it was not possible to make satisfactory inference with the available data. This inspired us to understand the model class better, to enable us to specify better prior distributions, and to explore the opportunity to use more data to learn about the underlying non-stationary process. In this paper,

we propose a framework for prior specification for the non-stationary SPDE based models with explanatory variables in the dependence structure. Further, we propose and test a model for annual precipitation that allows for replicates, such that multiple years of annual precipitation observations can be used to make inference. The replicate model is set up such that the model for one replicate corresponds to the model in [Ingebrigtsen et al. \(2014\)](#). Properties of the model and study system are explored in a simulation study.

This paper is organised as follows. In Section 2, we present the SPDE approach to spatial statistics and how this approach is used to define the non-stationary GRF model with spatial explanatory variables in the dependence structure. Section 3 presents annual precipitation data from southern Norway, the suggested replicate model for annual precipitation, prior specification for the SPDE parameters, and a brief outline of the inference procedure and model evaluation. The annual precipitation dataset is analysed in Section 4, and Section 5 presents the simulation study. We end the paper with a discussion in Section 6.

2 The SPDE approach to spatial statistics

Classical geostatistical models for point referenced data can easily become computer intensive as the computation time increases cubically with the number of observation locations. The computational bottleneck comes from the need to perform matrix operations with large and dense covariance matrices. For gridded data and for graph models, Gaussian Markov random fields (GMRF) have been used as computationally efficient alternatives, since they allow the computations to be carried out using a sparse precision matrix, i.e. the inverse of the covariance matrix ([Rue and Held, 2005](#)). [Lindgren et al. \(2011\)](#) suggest an approach where the two approaches are unified, by specifying a spatial Gaussian random field (GRF) model via a stochastic partial differential equation (SPDE) formulation instead of explicitly defining a covariance function. Many SPDE models are also Markov models, or can be approximated with Markov models, which means that the spatial model itself can be defined in continuous space, while the computations can be carried out efficiently due to properties of discrete GMRFs (see e.g. [Rue and Held, 2005](#)). However, it turns out that the benefits of the SPDE approach are not only computational; the SPDE formulation also provides a framework for introducing non-stationarity to the dependence structure ([Lindgren et al., 2011](#); [Bolin and Lindgren, 2011](#); [Ingebrigtsen et al., 2014](#); [Fuglstad et al., 2014b](#)).

The basis of the SPDE approach is the equation

$$(\kappa^2 - \Delta)^{\alpha/2}(\tau x(\mathbf{s})) = \mathcal{W}(\mathbf{s}), \quad \mathbf{s} \in \mathbb{R}^d, \quad (1)$$

whose stationary solutions $x(\mathbf{s})$ are GRFs with Matérn covariance functions for every $\alpha > d/2$, ([Whittle, 1954, 1963](#)) and GMRFs when α is an integer. In the formulation above, \mathcal{W} is spatial Gaussian white noise, Δ is the Laplacian, $\kappa > 0$

controls the spatial range, $\tau > 0$ controls the variance, and α controls the smoothness. The Matérn covariance function between locations \mathbf{s}_1 and \mathbf{s}_2 in \mathbb{R}^d is given by

$$C(\mathbf{s}_1, \mathbf{s}_2) = \frac{\sigma^2}{2^{\nu-1}\Gamma(\nu)} (\kappa \|\mathbf{s}_2 - \mathbf{s}_1\|)^\nu K_\nu(\kappa \|\mathbf{s}_2 - \mathbf{s}_1\|), \quad (2)$$

where K_ν is the modified Bessel function of the second kind and order $\nu > 0$, κ is a positive scaling parameter, and σ^2 is the marginal variance. The parameters in the SPDE and the Matérn covariance function of its solution are coupled; the smoothness parameter of the Matérn function is $\nu = \alpha - d/2$, and the marginal variance is

$$\sigma^2 = \frac{\Gamma(\nu)}{\Gamma(\alpha)(4\pi)^{d/2}\kappa^{2\nu}\tau^2}. \quad (3)$$

The SPDE above have stationary solutions with Matérn covariance. However, since properties of the random field can be characterised by an SPDE rather than a covariance function, we can modify the SPDE to obtain GRFs with more flexible dependence structures. One way to introduce more flexibility is allowing the parameters to change with location. Such local specification of parameters is possible due to the local nature of the differential operators.

The non-stationary SPDE based GRF model in [Ingebrigtsen et al. \(2014\)](#) is defined via

$$(\kappa(\mathbf{s})^2 - \Delta)(\tau(\mathbf{s})x(\mathbf{s})) = \mathcal{W}(\mathbf{s}), \quad \mathbf{s} \in \mathbb{R}^2, \quad (4)$$

which is a generalisation of the stationary model with $d = 2$ and $\alpha = 2$. The smoothness of the solutions depend on the smoothness of the non-stationary parameter functions. For piecewise continuous $\kappa(\mathbf{s})$ and $\tau(\mathbf{s})$, both bounded away from zero, the product $\tau(\mathbf{s})x(\mathbf{s})$ will have at least piecewise Hölder continuity $1 - \epsilon$ for any $\epsilon > 0$, corresponding to $\nu = 1$ in the stationary case. The continuity of $x(\mathbf{s})$ is then determined via the continuity of $\tau(\mathbf{s})$, since it acts as a direct and local scaling factor. Further, for deterministic basis functions $b_{\tau,j}(\cdot)$ and $b_{\kappa,j}(\cdot)$, and weight parameters $\boldsymbol{\theta}$, log-linear models for $\tau(\mathbf{s})$ and $\kappa(\mathbf{s})$ are given by

$$\log \tau(\mathbf{s}) = \theta_{\tau,1} + \sum_j b_{\tau,j}(\mathbf{s})\theta_{\tau,j}, \quad \log \kappa(\mathbf{s}) = \theta_{\kappa,1} + \sum_j b_{\kappa,j}(\mathbf{s})\theta_{\kappa,j}. \quad (5)$$

The basis functions can be spherical harmonics or B-splines as in [Lindgren et al. \(2011\)](#), or spatial explanatory variables as in [Ingebrigtsen et al. \(2014\)](#). Spatially rough explanatory variables may benefit from pre-smoothing, which in practice has the effect of moving some of the local structure into the observation noise.

The non-stationary SPDE based model has the computational advantages mentioned in the beginning of this section. It is possible to derive a GMRF approximation to the non-stationary GRF, which speeds up the computations considerably. The approximation is found using a finite element method (FEM) (see e.g. [Brenner and Scott, 2007](#)). The spatial domain is discretised into non-intersecting triangles

with m nodes and the approximation to the infinite dimensional GRF is built on the finite basis function representation

$$x(\mathbf{s}) = \sum_{i=1}^m \psi_i(\mathbf{s}) w_i, \quad (6)$$

with deterministic basis functions $\{\psi_i\}_{i=1,\dots,m}$ and weights $\mathbf{w} = (w_1, \dots, w_m)$. The approximation properties depend on the quality of the triangulation mesh (Lindgren et al., 2011), with generally increasing accuracy for decreasing triangle edge lengths. The Gaussian weights are chosen so that the representation in (6) approximates the distribution of the solution to the SPDE in (1) (in a stochastically weak sense). Lindgren et al. (2011) use piecewise polynomial basis functions with compact support to obtain a Markov approximation, and the sparse structure of the precision matrix \mathbf{Q} of \mathbf{w} is determined by the triangulation. The elements of \mathbf{Q} are functions of the θ 's in (5) that define the spatially varying covariance parameters τ and κ , i.e.

$$\mathbf{Q} = \mathbf{T}(\mathbf{K}^2 \mathbf{C} \mathbf{K}^2 + \mathbf{K}^2 \mathbf{G} + \mathbf{G} \mathbf{K}^2 + \mathbf{G} \mathbf{C}^{-1} \mathbf{G}) \mathbf{T}, \quad (7)$$

where \mathbf{T} and \mathbf{K} are diagonal matrices with $T_{ii} = \tau(\mathbf{s}_i)$ and $K_{ii} = \kappa(\mathbf{s}_i)$, and i is an index over the m nodes in the triangulation. The matrices \mathbf{C} and \mathbf{G} are finite element structure matrices, where \mathbf{C} is diagonal, with $C_{ii} = \int \psi_i(\mathbf{s}) d\mathbf{s}$, and \mathbf{G} is sparse positive semi-definite, with $G_{ij} = \int \nabla \psi_i(\mathbf{s}) \cdot \nabla \psi_j(\mathbf{s}) d\mathbf{s}$.

3 Annual precipitation: data, model, and inference

This section begins with a presentation of the annual precipitation data from southern Norway. Then, the stationary and non-stationary annual precipitation models that were compared in Ingebrigtsen et al. (2014) are extended to include data from multiple years. New conditions for prior specification of the dependence structure parameters are derived. Further, a brief outline of the inference procedure using integrated nested Laplace approximation (INLA, Rue et al., 2009) is given. The section ends with a presentation of how the models are evaluated.

3.1 Data

The data analysed in this paper is annual total precipitation in southern Norway. Daily precipitation observations from stations/gauges in the 16 counties south of and included Nord-Trøndelag, over the five year period 2008-09-01 – 2013-08-31, were obtained from eKlima, a database provided by the Norwegian Meteorological Institute (www.eKlima.no). Five annual datasets were created by aggregating the daily observations and removing stations with incomplete records. The five year dataset contains observations from 371 different stations. However, the number of stations, and which stations there are measurements from, varies from year to year. Table 1 contains a summary of the five year dataset. An elevation map with

Table 1: Five years of annual total precipitation data from southern Norway. The data are from the Norwegian Meteorological Institute’s database eKlima. The unit of the annual total precipitation is metres.

year	observations	mean	median	minimum	maximum
2008-2009	233	1.2778	1.0495	0.3560	3.6886
2009-2010	222	1.0091	0.8930	0.3055	2.8376
2010-2011	194	1.1825	0.9879	0.4008	3.5118
2011-2012	141	1.6450	1.2938	0.4051	4.5472
2012-2013	199	1.1393	0.9514	0.3120	3.4627

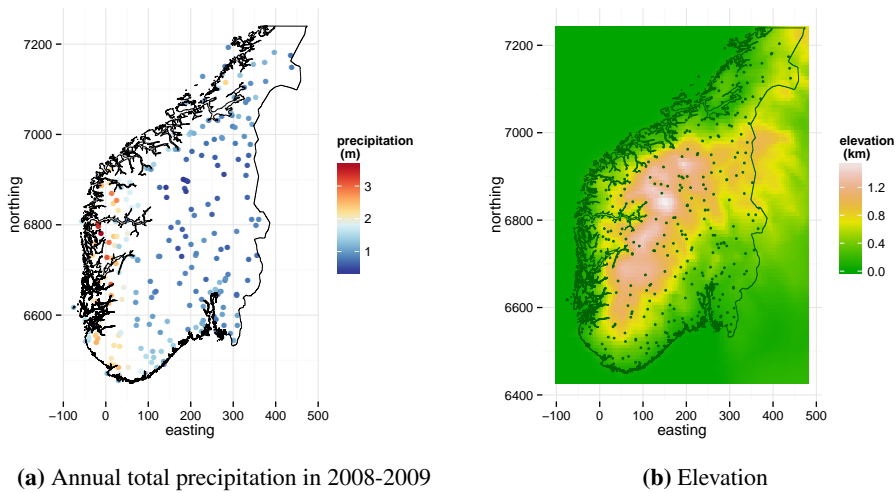


Figure 1: **1a)** Observations of annual total precipitation in 2008-2009 (from the Norwegian Meteorological Institute). **1b)** Smoothed elevation map of southern Norway (based on the digital elevation model GLOBE, [GLOBE Task Team, 1999](#)) with the 371 measurement locations indicated with dots. The coordinate reference system is UTM33 and distances are in km.

the locations of the 371 measurement stations, and a spatial plot of the annual total from 2008-2009, are found in Figure 1. The triangulation of the domain and the smoothed elevation model are the same as in Ingebrigtsen et al. (2014). The observed spatial pattern, with highest amounts of precipitation in western Norway, is characteristic for the Norwegian climate. Thus, the pattern seen in Figure 1a is similar for all of the years in the study. Consecutive years have fewer observations than 2008-2009. This is due to a combination of missing data and that several stations have been taken out of operation.

3.2 Precipitation model with replicates

Consider a spatial domain \mathcal{D} and n observation locations $\{s_1, \dots, s_n\}$ in \mathcal{D} , in our case, southern Norway and the locations of the Norwegian Meteorological Institute's weather stations in southern Norway. The observed annual total precipitation y_{ij} at station i and year j is modelled as

$$y_{ij} = \beta_j + \beta_h h(s_i) + x_j(s_i) + \epsilon_{ij}, \quad i = 1, \dots, n, \quad j = 1, \dots, r, \quad (8)$$

where β_j is a year specific intercept, $h(s_i)$ is the elevation at location s_i , and β_h is a linear effect of elevation, assumed to be common for all years. The spatial structure is incorporated through a zero mean GRF $x(s)$, which is modelled using the SPDE based model defined in Section 2 and has parameters θ . The spatial fields $x_j(s)$, $j = 1, \dots, r$, are assumed to be independent realisations, or replicates, of this GRF model. Additive measurement error is included as independent, identically distributed noise terms ϵ_{ij} . It is assumed that the ϵ_{ij} 's are independent of the other model components, and that they are normally distributed with zero mean and precision τ_ϵ .

One of the main objectives of this study is to gain insight into how the use of replicates influences the inference. Hence, the replicate model is set up such that the parameters have the same interpretation regardless of whether the model is fitted to only one realisation or to several replicates. The amount of precipitation differs between years (Table 1), therefore, the intercept is allowed to vary from year to year. If the model only had a common intercept, the between year variation would be captured by the random spatial term $x_j(s)$ and its parameters θ would not have the same interpretation with one realisation and with replicates. The linear effect of elevation in the mean β_h is modelled as common for all years because it is expected to be a coefficient related to the physical process.

An alternative model for observations from several years, would be to have two spatial terms: 1) a temporal constant field $c(s)$ that could be interpreted as the climatology, and 2) annual fields $x_j(s)$ to model the between year variation. This model would not be identifiable with one realisation. Furthermore, the spatial random term $x_j(s)$ have a different interpretation in this model than in the model in (8) since it describes spatial deviation from the climatology and not overall spatial variation. A model including the climatology term $c(s)$ can be useful if one wants to do forecasting or interpolate the climatology with uncertainty. In addition, the

model in (8) has only one explanatory variable (elevation), both in the mean and in the dependence structure. A simple model like this makes the results more transparent. However, if the main purpose was to predict and/or model precipitation it would be appropriate to search for more explanatory variables, e.g. other topographical variables such as aspect or surface roughness. Because our main focus is on estimation and the use of replicates, alternative models are not explored in this paper.

The GRF x in (8) is a solution to the SPDE (4), with dependence structure parameters θ as given in (5). We introduce models with different dependence structures for x : 1) A stationary model where the GRF has Matérn covariance and parameters $\theta_S = (\theta_\tau, \theta_\kappa)$,

$$\log \tau = \theta_\tau \quad \text{and} \quad \log \kappa = \theta_\kappa. \quad (9)$$

2) A non-stationary model where the GRF has parameters $\theta_{NS} = (\theta_{\tau,1}, \theta_{\tau,h}, \theta_{\kappa,1}, \theta_{\kappa,h})$, and elevation is included in the dependence structure as a log-linear effect on τ and κ

$$\log \tau(\mathbf{s}) = \theta_{\tau,1} + h(\mathbf{s}) \theta_{\tau,h} \quad \text{and} \quad \log \kappa(\mathbf{s}) = \theta_{\kappa,1} + h(\mathbf{s}) \theta_{\kappa,h}. \quad (10)$$

Note that the non-stationary model is stationary if $\theta_{\tau,h} = \theta_{\kappa,h} = 0$. We will use x_S to denote the stationary GRF and x_{NS} to denote the non-stationary GRF, and refer to the stationary and non-stationary precipitation models as the model in (8) with the GRF being stationary or non-stationary, respectively. However, the overall structure of the model does not change using the different GRF models, only the dependence structure of the SPDE based spatial model. Thus, if the subscript is not specified, we refer to both models.

To make the model identifiable, i.e. to separate the linear effects β_j and β_h from the spatial effect x_j , the following linear orthogonality constraints are imposed on the spatial fields

$$\int_{\mathcal{D}} x_j(\mathbf{s}) d\mathbf{s} = 0, j = 1, \dots, r, \quad (11)$$

$$\sum_{j=1}^r \int_{\mathcal{D}} h(\mathbf{s}) x_j(\mathbf{s}) d\mathbf{s} = 0. \quad (12)$$

This is known as restricted spatial regression (Hanks et al., 2015), and the constraints are imposed for both the stationary and the non-stationary model. Restricting the random field to be orthogonal to spatial covariates (here elevation) changes the interpretation of the spatial field to be a Bayesian version of restricted maximum likelihood; It is the spatial effect after the linear effect of elevation in the mean is accounted for. If precipitation data from only one year is used, i.e. $r = 1$, the replicate model in (8) corresponds to the model in Ingebrigtsen et al. (2014), and this model will be referred to as the individual model.

Inference with the annual precipitation models is carried out under the Bayesian paradigm. Thus, prior distributions need to be specified for all model parameters,

i.e. the regression coefficients $\beta_1, \dots, \beta_r, \beta_h$, the precision of the measurement error τ_ϵ , and the dependence structure parameters θ . For the regression parameters we use vague Gaussian priors; all β 's are $\mathcal{N}(0, 100^2)$. The measurement error precision τ_ϵ is Gamma distributed with shape parameter 2 and rate parameter 0.02. Prior specification for θ follows in the next section.

3.3 Prior specification for SPDE parameters

Assigning priors to the SPDE parameters θ_S and θ_{NS} is a bit intricate; they control the spatial dependence structure, but do not have a direct physical interpretation. Further, the simulation study in [Ingebrigtsen et al. \(2014\)](#) demonstrated the difficulty of estimating covariance parameters based on one realisation of the spatial field. The spatial correlation range parameters, $\theta_{\kappa,1}$ and $\theta_{\kappa,h}$, used to sample datasets were not well recovered, and the posterior credible interval coverages were as low as 5% and 26% for $\theta_{\kappa,1}$ and $\theta_{\kappa,h}$, respectively. The coverage was higher for $\theta_{\tau,1}$ and $\theta_{\tau,h}$; 84% for both parameters. In addition to low coverage, there was bias towards the prior means, which indicates prior sensitivity and show that priors for θ_{NS} should be chosen with care, and not be too informative. Also, since the stationary and non-stationary models are compared, priors in the two models should be based on similar assumptions about the dependence structure of the underlying spatial process.

For the stationary GRF with Matérn covariance and smoothness parameter $\nu = 1$, the marginal standard deviation is given by

$$\sigma_S = 1/(\sqrt{4\pi\tau\kappa}), \quad (13)$$

and we define the spatial correlation range to be

$$\rho_S = \sqrt{8}/\kappa. \quad (14)$$

With ρ_S defined as above, this is the distance where the correlation has dropped to 0.13.

Recall from (9) that $\theta_\tau = \log \tau$ and $\theta_\kappa = \log \kappa$. We assume a priori that $\theta_\tau \sim \mathcal{N}(\mu_\tau, \sigma_\tau^2)$ and $\theta_\kappa \sim \mathcal{N}(\mu_\kappa, \sigma_\kappa^2)$, and that θ_τ and θ_κ are independent. The parameters $(\mu_\tau, \sigma_\tau^2)$ and $(\mu_\kappa, \sigma_\kappa^2)$ need to be specified. However, since we have knowledge about the magnitude of the annual total precipitation and distances in southern Norway, it would be easier to specify prior parameters for the distributions of σ_S and ρ_S rather than for θ_τ and θ_κ . From properties of the log-normal distribution it follows that

$$\rho_S \sim \log \mathcal{N}(\log \sqrt{8} - \mu_\kappa, \sigma_\kappa^2),$$

and

$$\sigma_S \sim \log \mathcal{N}(-\log \sqrt{4\pi} - \mu_\tau - \mu_\kappa, \sigma_\tau^2 + \sigma_\kappa^2).$$

The p -quantiles of the log-normal distributions for the correlation range and marginal standard deviation are

$$\rho_S(p) = \sqrt{8} \exp(-\mu_\kappa + \sigma_\kappa \Phi^{-1}(p)),$$

and

$$\sigma_S(p) = \frac{1}{\sqrt{4\pi}} \exp(-\mu_\tau - \mu_\kappa + \sqrt{\sigma_\tau^2 + \sigma_\kappa^2} \Phi^{-1}(p)),$$

where $0 \leq p \leq 1$, and $\Phi(\cdot)$ is the cumulative distribution function for the standard normal distribution. To choose priors we can now specify two quantiles of ρ_S and σ_S , e.g. the median and 0.9-quantile, and then solve the corresponding four equations for $(\mu_\tau, \sigma_\tau^2)$ and $(\mu_\kappa, \sigma_\kappa^2)$.

The relationships between the marginal standard deviation and correlation range, and the SPDE parameters τ and κ in (13) and (14) are only valid in the stationary case. In the non-stationary case, we can obtain nominal approximations for $\sigma_{NS}(h)$ and $\rho_{NS}(h)$ as functions of the elevation $h = h(\mathbf{s})$. Similar to the stationary case, the Gaussian priors are assigned to θ_{NS} such that

$$\begin{aligned} \theta_{\tau,1} &\sim \mathcal{N}(\mu_{\tau,1}, \sigma_{\tau,1}^2), & \theta_{\tau,h} &\sim \mathcal{N}(\mu_{\tau,h}, \sigma_{\tau,h}^2), \\ \theta_{\kappa,1} &\sim \mathcal{N}(\mu_{\kappa,1}, \sigma_{\kappa,1}^2), & \theta_{\kappa,h} &\sim \mathcal{N}(\mu_{\kappa,h}, \sigma_{\kappa,h}^2). \end{aligned}$$

The θ 's are assumed to be independent, which yields the following marginal prior distributions of the nominal range and nominal standard deviation at elevation h

$$\rho_{NS}(h) \sim \log \mathcal{N}(\log \sqrt{8} - \mu_{\kappa,1} - h\mu_{\kappa,h}, \sigma_{\kappa,1}^2 + h^2\sigma_{\kappa,h}^2),$$

and

$$\sigma_{NS}(h) \sim \log \mathcal{N}(-\log \sqrt{4\pi} - \mu_{\tau,1} - \mu_{\kappa,1} - h(\mu_{\tau,h} + \mu_{\kappa,h}), \sigma_{\tau,1}^2 + \sigma_{\kappa,1}^2 + h^2(\sigma_{\tau,h}^2 + \sigma_{\kappa,h}^2)),$$

where $h = h(\mathbf{s})$.

The non-stationary nominal prior distributions change with elevation. To make them similar to the stationary prior distributions we set up the following coherence conditions;

1. $\sigma_{NS}(0) \stackrel{d}{=} \sigma_S$ and $\rho_{NS}(0) \stackrel{d}{=} \rho_S$,
2. $\mu_{\tau,h} = \mu_{\kappa,h} = 0$,
3. given a reference elevation h_0 , c_ρ is the coefficient of variation for the ratio $\rho_{NS}(h_0)/\rho_{NS}(0)$, and c_σ is the coefficient of variation for the ratio $\sigma_{NS}(h_0)/\sigma_{NS}(0)$.

Here, h_0 , c_ρ , c_σ , σ_S , and ρ_S are used to define the prior for θ_{NS} . The first condition states that the stationary prior distributions and the non-stationary nominal prior distributions are equal at sea level. The second condition has two interpretations: i) the medians of the non-stationary prior distributions for the nominal range and standard deviation are invariant to elevation, ii) the priors are centred around no

influence, i.e. a priori we do not make any assumption of which effect elevation has on the spatial correlation range and marginal standard deviation. The third condition is introduced to control how much the priors are allowed to change with elevation. We look at the relative change in $\rho_{\text{NS}}(h)$ and $\sigma_{\text{NS}}(h)$ from sea level to a chosen reference elevation h_0 , and control the change by specifying the coefficients of variation.

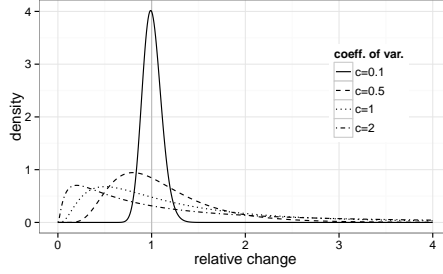
From the three coherence conditions and the stationary prior parameters $(\mu_\tau, \sigma_\tau^2)$ and $(\mu_\kappa, \sigma_\kappa^2)$, it follows that

$$\begin{aligned}\mu_{\tau,1} &= \mu_\tau, & \sigma_{\tau,1}^2 &= \sigma_\tau^2, \\ \mu_{\tau,h} &= 0, & \sigma_{\tau,h}^2 &= \frac{1}{h_0^2} \log\left(\frac{c_\sigma^2 + 1}{c_\rho^2 + 1}\right), \\ \mu_{\kappa,1} &= \mu_\kappa, & \sigma_{\kappa,1}^2 &= \sigma_\kappa^2, \\ \mu_{\kappa,h} &= 0, & \sigma_{\kappa,h}^2 &= \frac{1}{h_0^2} \log(c_\rho^2 + 1),\end{aligned}$$

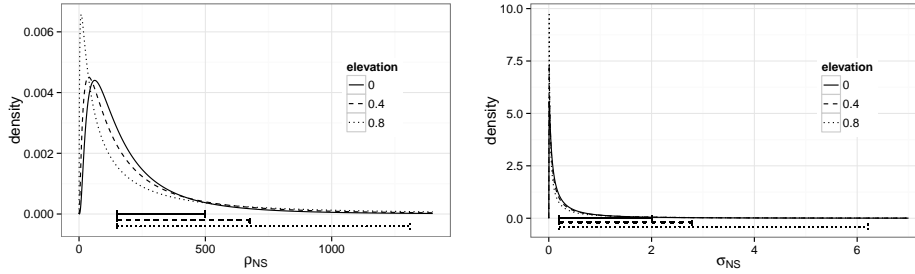
for a given reference elevation h_0 and coefficients of variation c_σ and c_ρ . To ensure positive variance, $c_\sigma > c_\rho$, i.e. the relative change in $\sigma_{\text{NS}}(h)$ needs to be allowed to vary more than the relative change in $\rho_{\text{NS}}(h)$.

The coefficients of variation are used to set the prior variance for the non-stationarity parameters $\theta_{\tau,h}$ and $\theta_{\kappa,h}$. In the limiting case, when c_σ and c_ρ approach zero, the prior variances also approach zero, and the model is essentially assumed to be stationary. Increasing the coefficients of variance, means increasing the prior variance. The relative changes in nominal range and standard deviation are log-normally distributed, i.e. $\rho_{\text{NS}}(h_0)/\rho_{\text{NS}}(0) \sim \log \mathcal{N}(0, \log(c_\sigma^2 + 1))$ and $\sigma_{\text{NS}}(h_0)/\sigma_{\text{NS}}(0) \sim \log \mathcal{N}(0, \log(c_\rho^2 + 1))$. The medians of both ratios are one, thus, the distributions are centred around no change. Figure 2a show the density for $\rho_{\text{NS}}(h_0)/\rho_{\text{NS}}(0)$ and $\sigma_{\text{NS}}(h_0)/\sigma_{\text{NS}}(0)$ for different values of the coefficient of variation (c). When $c = 0.1$, the density is narrow and close to symmetric around one. Increasing c , increases the prior probability that the range/standard deviation is e.g. doubled/halved from sea level to h_0 . Note that similar approaches for prior specification can be applied to any type of explanatory variable.

The analysis domain, southern Norway, is approximately 500 km \times 700 km. We set the prior median range (ρ_S) to 150 km and 0.9-quantile to 500 km. This yields $\mu_\kappa = -3.97$ and $\sigma_\kappa^2 = 0.88$. Further, after considering the variation in the precipitation data, the prior median standard deviation (σ_S) is set to 0.2 m and 0.9-quantile to 2 m, giving $\mu_\tau = 4.31$ and $\sigma_\tau^2 = 2.35$. The average value of the smoothed elevation model is close to 0.4 km, and this value is used as the reference elevation h_0 . We set $c_\rho = 0.8$ and $c_\sigma = 1.3$, and get $\sigma_{\tau,h}^2 = 3.09$ and $\sigma_{\kappa,h}^2 = 3.09$. The prior densities for $\rho_{\text{NS}}(h)$ and $\sigma_{\text{NS}}(h)$, for this choice of parameters, and at different elevations h , can be seen in Figure 2. The prior values are chosen as a compromise between having wide enough priors, but narrow enough to restrict the prior range not to be too long. Having a $\mathcal{N}(0, 3.09)$ -prior for $\theta_{\kappa,h}$ might seem



(a) Density of the relative change in the non-stationary nominal priors from sea level to h_0 for different values of coefficient of variation.



(b) Prior density of $\rho_{NS}(h)$ when $h = 0, h_0, 2h_0$. (c) Prior density of $\sigma_{NS}(h)$ when $h = 0, h_0, 2h_0$.

Figure 2: 2a) is the density of the relative changes $\rho_{NS}(h_0)/\rho_{NS}(0)$ and $\sigma_{NS}(h_0)/\sigma_{NS}(0)$ for different values of the coefficient of variation. 2b) and 2c) are the prior densities for $\rho_{NS}(h)$ and $\sigma_{NS}(h)$ at different elevations h . The reference elevation h_0 is 0.4 km, and the coefficients of variation are $c_\rho = 0.8$ and $c_\sigma = 1.3$. The 0.5- and 0.9-quantiles at sea level are set to 150 km and 500 km for ρ_{NS} , and 0.2 m and 2 m for σ_{NS} . The intervals given by the 0.5- and 0.9-quantiles are indicated with horizontal lines at the bottom of the plots.

strict. However, in Figure 2b it can be seen that the 0.9-quantile of ρ_{NS} at $h = 0.8$ is around 1300 km, i.e. almost two times the length of the domain.

3.4 Bayesian inference with R-INLA

The annual precipitation models are fitted under the Bayesian paradigm and target for the inference are posterior predictive distributions at spatial locations of interest and posterior distributions for $\beta_1, \dots, \beta_r, \beta_h, \tau_e$, and θ . The prior distributions assigned to these model parameters were specified in Sections 3.2 and 3.3. In addition, the weight vector w from the basis representation of the GRF in (6) is assigned a GMRF prior with precision matrix as in (7). The stationary and non-stationary precipitation models fit into the latent Gaussian model framework from Rue et al. (2009) and approximations to the posterior marginal densities, posterior predictive densities as well as measures of model fit can be obtained with integrated nested Laplace approximation (INLA). In fact, because the likelihood is Gaussian,

the approximations are exact up to numerical integration error.

We refer to [Ingebrigtsen et al. \(2014, Section 4.5\)](#) for details on inference with our precipitation models using INLA, and to [Lindgren and Rue \(2014\)](#) for a thorough introduction to Bayesian spatial modelling with the SPDE approach and INLA. Both the INLA methodology and SPDE based spatial models are available in R ([R Core Team, 2013](#)), in the R package `R-INLA` (see www.r-inla.org). All inference was carried out using this software.

3.5 Model evaluation

To assess how well each model fits the observations, we use the deviance information criterion (DIC, [Spiegelhalter et al., 2002](#)). DIC is a model selection tool for Bayesian hierarchical models. It is a measure that combines goodness-of-fit in terms of deviance and complexity in terms of effective number of parameters. The deviance is defined as $D = -2 \log L$, where L is the likelihood. DIC is given by the expression

$$\text{DIC} = \bar{D} + p_D.$$

\bar{D} is the expectation of the deviance over the posterior distribution. The effective number of parameters p_D is the posterior mean deviance minus the deviance of the posterior mean of the parameters. Models with smaller DIC have better support in the data. A commonly used rule of thumb is that a difference in DIC greater than ten is considered a significant difference. DIC has been criticised, but is also frequently used (see [Spiegelhalter et al. \(2014\)](#) for a summary). DIC performed very well for selecting the correct model in the simulation study in [Ingebrigtsen et al. \(2014\)](#), so we choose to evaluate model fit of the stationary and non-stationary precipitation models with DIC. Refer to [Holand et al. \(2013\)](#) for a description of how DIC is computed in `R-INLA`.

To evaluate predictive performance we run leave-one-out cross-validation. All annual observations at one station are held out of the analysis and the remaining stations are used for both model fitting and interpolating/predicting the amount of precipitation, for each year, at the location of the removed station. This is repeated for all 371 stations. We compute the the root mean square error (RMSE) for each year

$$\text{RMSE}_j = \sqrt{\frac{1}{n_j} \sum_{i=1}^{n_j} (\hat{y}_{ij} - y_{ij})^2},$$

where n_j is the number of observations in year j , y_{ij} is the observation at station i and year j , and \hat{y}_{ij} is the mean of the posterior predictive distribution when the model was fitted to data from all stations except station i . As a summary score we use the average RMSE

$$\overline{\text{RMSE}} = \frac{1}{r} \sum_{j=1}^r \text{RMSE}_j.$$

In addition to RMSE, we compute the continuous ranked probability score (CRPS), which unlike RMSE assesses the whole posterior predictive distribution, and not only the predictive mean. CRPS is defined as

$$\text{CRPS}(F, y) = \int_{-\infty}^{\infty} (F(u) - 1\{y \leq u\})^2 du,$$

where F is the predictive cumulative distribution function and y is the observed value (Gneiting and Raftery, 2007). Both RMSE and CRPS are on the same scale as the observations, i.e. metres in our case. Similarly to for RMSE, we define the average CRPS as

$$\overline{\text{CRPS}} = \frac{1}{r} \sum_{j=1}^r \frac{1}{n_j} \sum_{i=1}^{n_j} \text{CRPS}(F_{ij}, y_{ij}),$$

where F_{ij} is the leave-one-out posterior predictive cumulative distribution function for observation y_{ij} .

The true leave-one-out posterior predictive distribution for each y_{ij} is a continuous Gaussian mixture, but to simplify the numerical calculations, the predictive distributions are approximated with a Gaussian distribution, which allows CRPS to be computed analytically with the function available in the R-package *verification* (NCAR - Research Applications Laboratory, 2014). The approximation uses the leave-one-out posterior mean \hat{y}_{ij} of the linear predictor $\eta_{ij} = \beta_j + \beta_h h(\mathbf{s}_i) + x_j(\mathbf{s}_i)$, and the predictive variance is taken to be the sum of the leave-one-out posterior variance of η_{ij} and the posterior expectation of the observation noise variance $1/\tau_\epsilon$. Hence, the uncertainty of all parameters except τ_ϵ is integrated out.

4 Data analysis

Table 2: Difference in deviance information criterion (DIC) when the annual precipitation models were fitted with stationary and non-stationary dependence structures. Individual models were fitted to the five years separately, and replicate models to all five years. ΔDIC is defined as DIC for the stationary model minus DIC for the non-stationary model.

model year(s)	individual 2008-2009	individual 2009-2010	individual 2010-2011	individual 2011-2012	individual 2012-2013	replicate 2008-2013
ΔDIC	55	51	90	10	7	159

The stationary and non-stationary replicate models from Section 3.2, with the priors specified in Section 3.3, were fitted to the southern Norway annual precipitation data from 2008-2013. Five years of observations are available, so the number of replicates r is five. For comparison, individual models ($r = 1$) were fitted to the five years separately. Table 2 contains the difference in DIC between the stationary

Table 3: Model predictions evaluated with leave-one-out cross-validation. Reported is CRPS averaged over stations and years, and RMSE averaged over years.

	CRPS		RMSE	
	stationary	non-stationary	stationary	non-stationary
individual models	0.14360	<i>0.13816</i>	0.26555	<i>0.25315</i>
replicate model	0.14377	0.14358	0.26456	0.25672

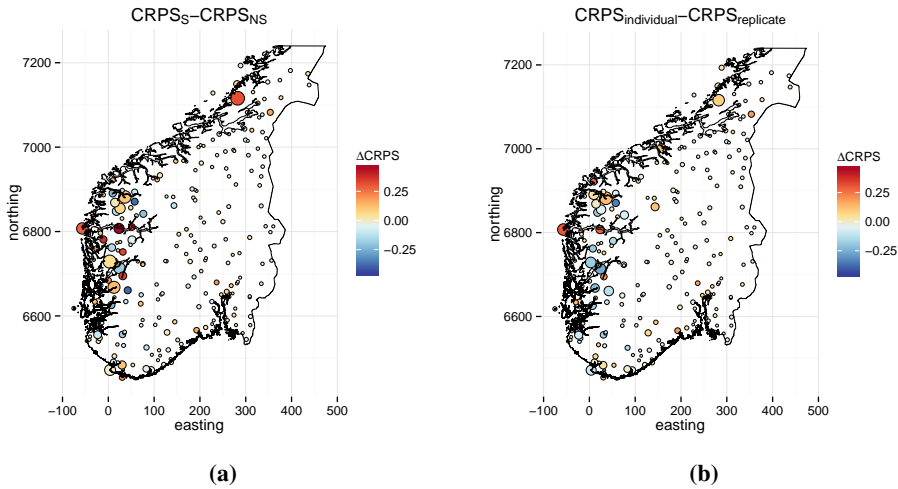


Figure 3: Maps of CRPS in 2008-2009 at each of the 233 weather stations computed with leave-one-out cross-validation. The colour scale indicates the difference in CRPS between stationary and non-stationary dependence structures in the replicate model (3a), and between using the non-stationary individual model and non-stationary replicate model (3b). The size of the points indicates the magnitude of the CRPS (average of the two models compared). Smaller size means better predictions.

and non-stationary models. DIC favours a non-stationary dependence structure for the replicate model and all individual models, although the difference is small for 2011-2012 and 2012-2013.

The main motivation for introducing non-stationarity with elevation as an explanatory variable in the dependence structure, was to improve spatial prediction of precipitation in difficult and mountainous terrain. Predictive performance is evaluated using the leave-one-out cross-validation described in Section 3.5. Table 3 contains CRPS averaged over stations and the five years, and RMSE averaged over the five years. The best prediction results are obtained when individual models with non-stationary dependence structure are fitted to each annual dataset separately. The non-stationary replicate model is ranked second best according to both RMSE and CRPS, but the difference in average CRPS between the non-stationary replicate model and stationary individual models is minimal.

The differences in average CRPS are small. However, looking at CRPS values at individual stations shows that the picture is more complex. The differences are much higher than the average suggests because one model is not uniformly better

at all stations. Figure 3 compares CRPS when different dependence structures were used in the replicate model (3a), and when the replicate or individual model were used and the dependence structure was non-stationary (3b). The spatial plots are for the year 2008-2009, and the difference in CRPS at each station is indicated with colour, while the size of the circles indicates the magnitude of the CRPS.

The largest circles, hence largest CRPS values, are located in western Norway, i.e. this is where the predictions miss the most. This is also where the amount of precipitation is high, and the topography is complex. In 2008-2009, the non-stationary replicate model has lower CRPS than the stationary replicate model at 48% of the stations, this is where the circles are filled with red. For the individual model this number is 57%. Many of the circles filled with red are located at difficult locations in western Norway, but the picture is not clear and there are locations at the west coast where the stationary model gives better predictions than the non-stationary model. The difference in CRPS between the individual and replicate models is smaller than the difference between dependence structures. The individual model is better at 62% of the stations in 2008-2009. This is where the circles are filled with blue in Figure 3b.

DIC, $\overline{\text{CRPS}}$, and $\overline{\text{RMSE}}$ all favour a non-stationary dependence structure. The non-stationary model will therefore be in focus for the rest of this section. Using annual precipitation data from more years did not improve predictions. However, it is not surprising that the individual model fitted to one annual dataset is better at predicting the amount of precipitation that particular year. Recall that the motivation for introducing non-stationarity was a more physics based model and possible improved predictions, but the motivation for introducing replicates was preciser estimates with better statistical properties (less biased and prior sensitive) for the dependence structure parameters.

Figure 4 show the posterior marginal densities for θ_{NS} when individual models were fitted to the annual data, and when the replicate model was fitted to all five years. The posterior marginal densities with the replicate model are narrower than the individual posteriors, i.e. the estimates have higher precision. Also, the replicate posteriors for $\theta_{\tau,1}$, $\theta_{\tau,h}$, and $\theta_{\kappa,h}$ are centred among the individual priors; the replicate model produces a kind of average estimate. The situation is different for $\theta_{\kappa,1}$. For this parameter, the replicate posterior is shifted away from the prior mean (-3.97) and towards smaller values and longer spatial correlation range at sea level.

From Figure 4c it seems like the posterior marginals from the individual models are shifted towards the prior mean. We investigate this further by fitting the non-stationary individual models and replicate model with an informative prior and a vague prior. The prior mean values are kept fixed, but the variances are decreased/increased by changing the 0.9-quantiles of ρ_S and σ_S , and the coefficients of variation c_ρ and c_σ . For the informative prior, the 0.9-quantile of ρ_S is set to 300 km, and the 0.9-quantile of σ_S is set to 0.5 m. Further, $c_\rho = 0.2$ and $c_\sigma = 0.3$. For the vague prior, the 0.9-quantiles are 800 km and 4 m, and $c_\rho = 2$ and $c_\sigma = 6$. In Figure 5, posteriors from models with the different priors are compared. We also compare posteriors from the individual model fitted to the 2008-2009 observations,

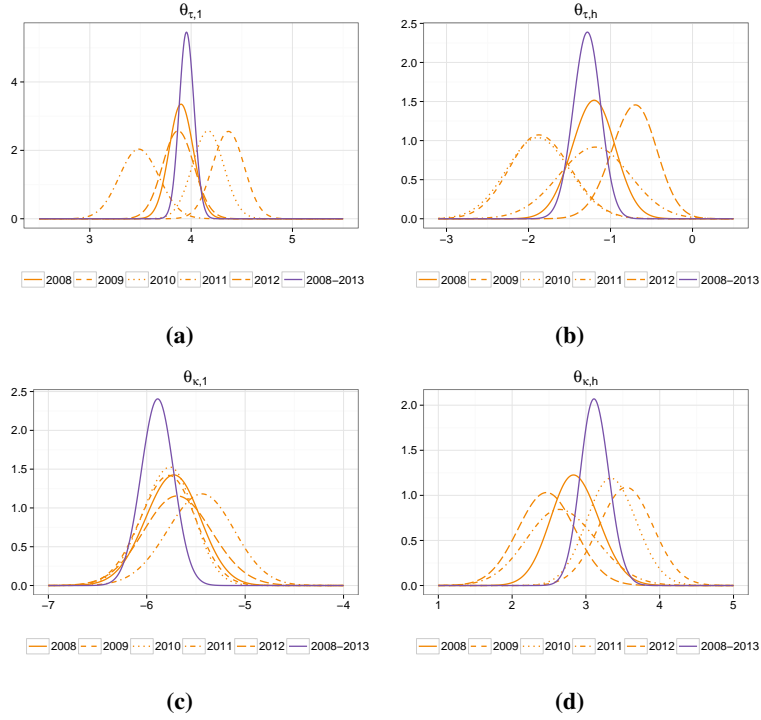


Figure 4: Posterior marginal densities for the dependence structure parameters θ_{NS} in the non-stationary precipitation model. The individual model was fitted to each annual dataset and the replicate model was fitted to the five years together.

and posteriors from the replicate model fitted to the 2008-2013 observations.

The dependence structure parameters are more sensitive to the choice of priors when there are no replicates of the spatial field. Also, the range parameters $\theta_{\kappa,1}$ and $\theta_{\kappa,h}$ are less robust than the variance parameters $\theta_{\tau,1}$ and $\theta_{\tau,h}$. In Figure 6 we show how the estimated spatial correlation range is influenced by different priors. With the individual model (panels 6a-6c) the prior is very influential on the spatial correlation. At sea level, the difference in correlation range is longer than the domain. With the replicate model (panels 6d-6f), the difference is much smaller.

A small study of the sensitivity with respect to c_ρ and c_σ can be found in Appendix B. The conclusion is that both estimates and cross-validated predictive scores are robust to the choices of c_ρ and c_σ .

5 Simulation study

The purpose of this simulation study is to investigate statistical properties of the spatial replicate model for annual precipitation. Parameter estimates and spatial predictions are assessed when increasing number of replicates of the spatial field are used for inference. Datasets are sampled from both the stationary and non-

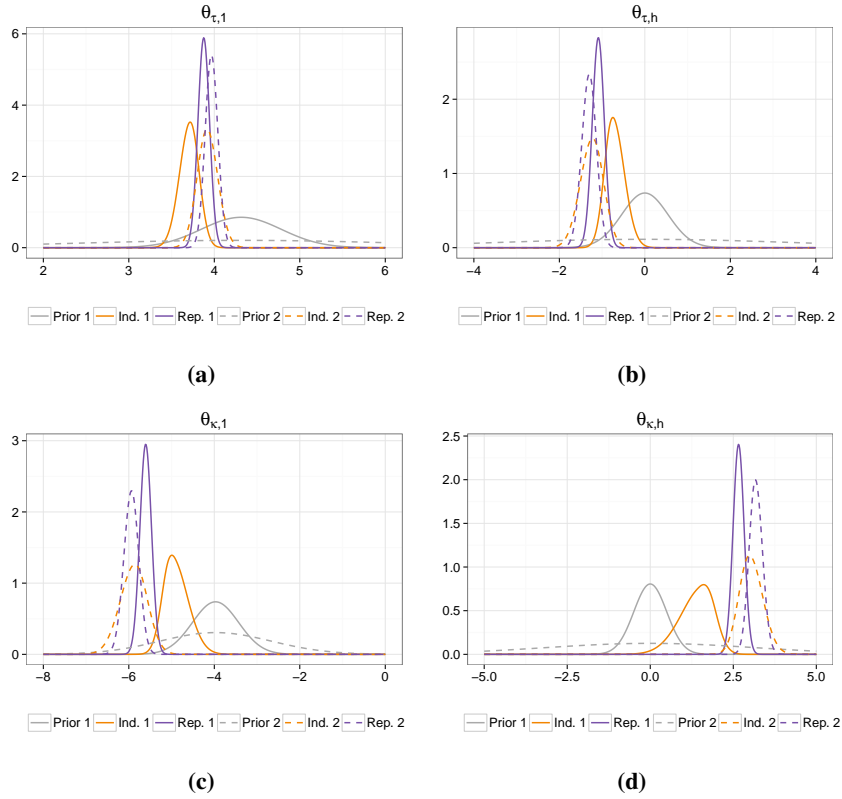


Figure 5: Posterior marginal densities for θ_{NS} when two different priors were used: 1) informative (solid lines) and 2) vague (dashed lines). Posterior marginals with the individual model (data: 2008-2009) are in orange and replicate model (data: 2008-2013) in purple. The priors are in grey.

stationary models, and models with both dependence structures are fitted to all datasets. The sampled fields respect the identifiability constraints in (11) and (12), by use of the general constrained sampling methods from Rue and Held (2005). We investigate how well DIC performs as a model choice criterion, and evaluate how well the true parameters are recovered by looking at posterior mean values, credible interval coverage, and RMSE. Further, we compare predictive performance of the stationary and non-stationary models as a function of the number of replicates, as well as pointwise in space.

5.1 Set-up

Annual precipitation datasets were sampled from the replicate model defined in Section 3.2, with both stationary and non-stationary dependence structures. The spatial domain, triangulation, and smoothed elevation model were the same as in the data analysis section (Section 4). We used the 233 stations from the 2008-2009 dataset as observation locations. The chosen parameter values are based on the analysis of the southern Norway data: The year specific intercepts $\beta_1, \beta_2, \dots, \beta_r$

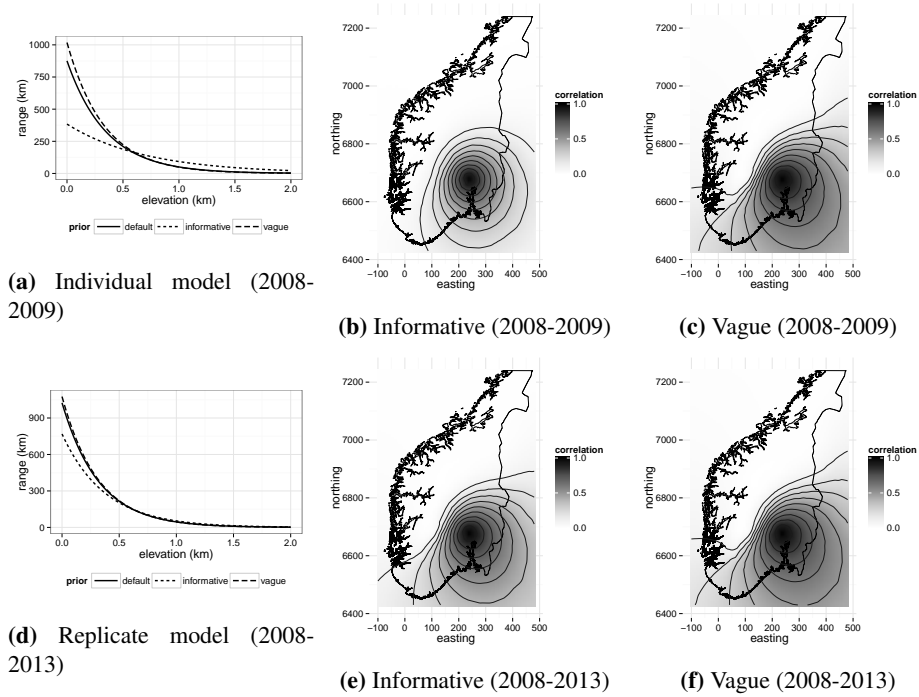


Figure 6: Spatial correlation range as a function of elevation, and between a reference location south-east in Norway and all other locations in the domain. Individual model in panel 6a-6c and replicate model in panel 6d-6f. Comparison between the informative and vague priors. The default prior referred to in panel 6a and 6d is the one defined in Section 3.3.

were given a common value of $\beta_0 = 0.6$, the linear effect of elevation was set to $\beta_h = 0.4$, and the precision of the measurement error was set to $\tau_\epsilon = 40$. These parameters were equal for the stationary and non-stationary datasets. The dependence structure parameters were set to $\theta_S = (3.5, -4.5)$ to obtain datasets based on stationary spatial fields, and $\theta_{NS} = (3.9, -1.3, -5.9, 3.1)$ to obtain datasets based on non-stationary spatial fields.

We assume we have data from r years at the 233 stations, and let the number of replicates r range from one to ten. The results we present in the next section are based on 250 sampled datasets. For $r = 1$ this means 250 annual datasets. However, for $r > 1$, one dataset means r annual datasets, so in total we sample $250 \times r$ sets of observations.

The stationary and non-stationary models with the priors defined in Section 3.3 were fitted to all sampled datasets, i.e. r sets of annual total precipitation observations at the 233 stations with the underlying fields being both stationary and non-stationary. The fitted models were used to predict annual total precipitation on the entire spatial domain (on the triangulation) and the predictions were compared to the sampled precipitation fields. Results follow in the next section, and in Appendix A.

5.2 Results

Figure 7 contains boxplots of ΔDIC , defined as DIC of the stationary model minus DIC of the non-stationary model. In the left panel (7a) the datasets are sampled from the stationary model and in the right panel (7b) from the non-stationary model. The model with the lowest DIC should be preferred and a rule of thumb is that a complex model should be preferred over a simpler model if the difference is greater than ten. We have indicated $\Delta\text{DIC} = 10$ with a horizontal line and note that DIC almost always favour the correct model. Note also that when the datasets are non-stationary, the ability to select the correct model improves when the number of replicates increases. When the datasets are from the non-stationary model, the misclassification rate is 0.16 for one replicate, 0.05 for two replicates, one dataset is misclassified when $r = 4$, and zero for all other values of r .

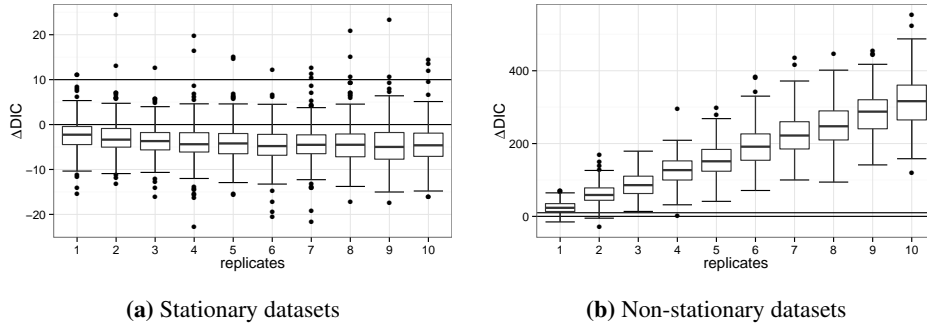


Figure 7: Box plots of the difference in DIC as a function of the number of replicates. Stationary and non-stationary models were fitted to datasets sampled from the stationary model (7a) and non-stationary model (7b). ΔDIC is the DIC of the stationary model minus DIC of the non-stationary model. ΔDIC of zero and ten are indicated with horizontal lines.

The rest of this section will focus on results when the datasets are sampled from a non-stationary model, and on the dependence structure parameters θ_{NS} . Results for the other parameters; β_0 , β_h , and τ_ϵ , and results when the true model is stationary can be found in Appendix A. In Figure 8 we have plotted the average of the posterior mean values for $\theta_{\tau,1}$, $\theta_{\tau,h}$, $\theta_{\kappa,1}$, and $\theta_{\kappa,h}$ estimated from the 250 datasets. The shaded areas indicate the range of the posterior mean values over all simulations. The overall trend is that the average values approach the true values when the number of replicates increases and the posterior mean values become more concentrated around the truth. The stationary model with dependence structure parameters θ_τ and θ_κ is, as expected, not able to recover the non-stationary parameters $\theta_{\tau,1}$ and $\theta_{\kappa,1}$ and using replicates does not reduce the bias. However, in Figure 15 in Appendix A.3 it can be seen that the non-stationary model is able to adapt to the stationary datasets.

The parameters related to the marginal variance, $\theta_{\tau,1}$ and $\theta_{\tau,h}$, are better recovered than the spatial range parameters $\theta_{\kappa,1}$ and $\theta_{\kappa,h}$. This can also be seen in Figure 9, which shows 95% posterior credible interval coverage and RMSE for θ_{NS} .

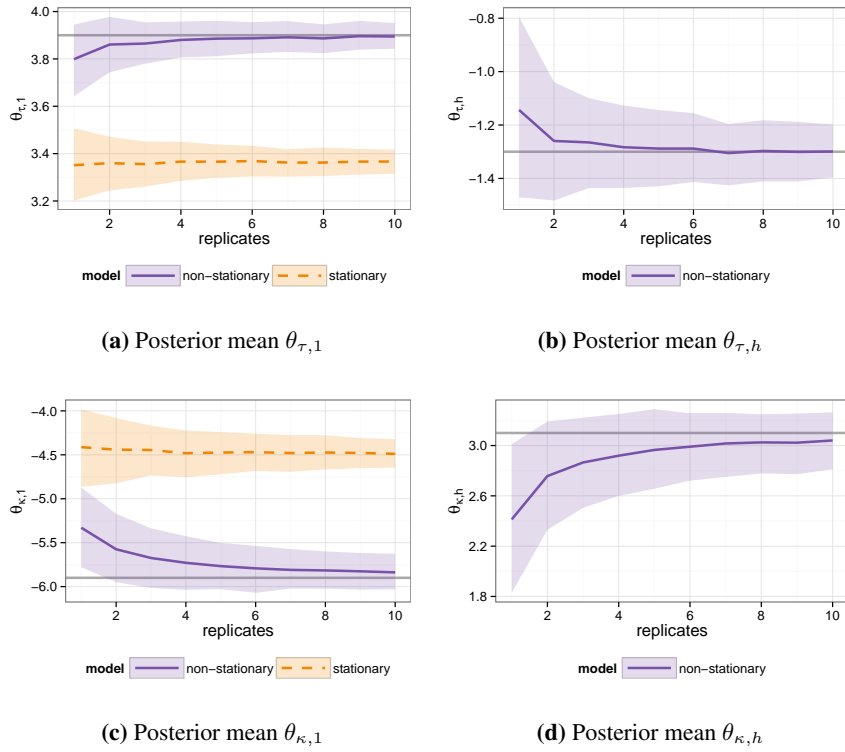


Figure 8: Stationary and non-stationary replicate models were fitted to datasets sampled from the non-stationary model. Presented are the posterior mean values for the spatial dependence structure parameters θ_S and θ_{NS} . The lines are averages over all datasets, while the shaded area span the range of the posterior mean values (between the 0.1- and 0.9-quantiles). The true parameter values are indicated with grey lines.

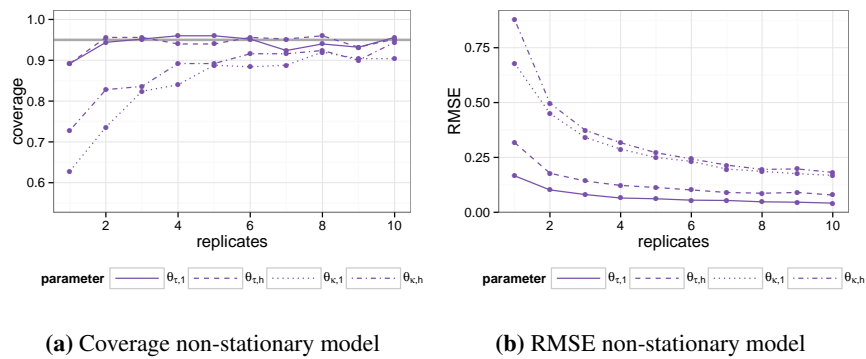


Figure 9: Non-stationary replicate models were fitted to datasets sampled from the non-stationary model. Presented are 95% posterior credible interval coverage and RMSE for the spatial dependence structure parameters θ_{NS} .

The coverage is as low as 63% for $\theta_{\kappa,1}$ when only one replicate of the field is used, but increases to 74% when the number of replicates is two. Adding more replicates increases the coverage and reduces RMSE. However, the largest improvement is between one and two replicates.

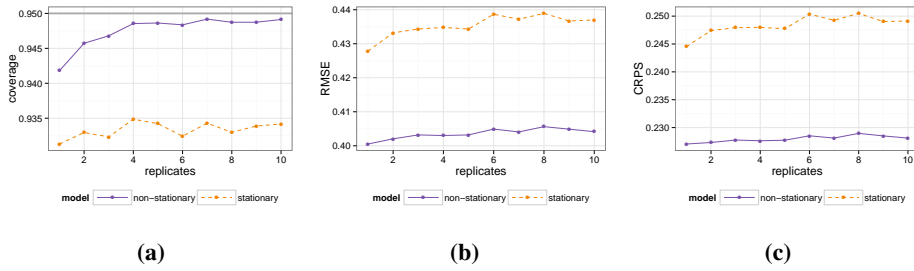


Figure 10: Stationary and non-stationary replicate models were fitted to datasets sampled from the non-stationary replicate model. Spatial predictions at the locations of the nodes of the triangulated domain are compared to the sampled fields. Predictive scores; coverage, RMSE, and CRPS, are averaged over all nodes.

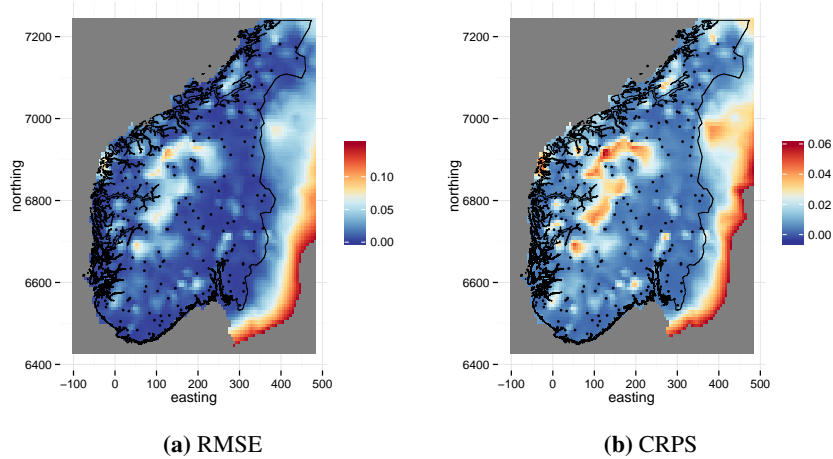


Figure 11: Predictive performance for simulated data. The figures show difference in RMSE and CRPS: stationary model minus non-stationary model, when the true model is non-stationary and $r = 5$. The presented spatial fields are pointwise averages over all replicates.

In addition to parameter estimates, we evaluate the predictive performance. With real data it is only possible to evaluate predictions at locations with observations. With simulated data we can investigate prediction properties at arbitrary locations since we are no longer restricted to know the truth only at the given stations. Thus, it is possible to evaluate how the models perform out-of-sample differently than any hold-out cross-validation allows. For us it is particularly interesting to investigate the behaviour in mountain areas with no observations.

For each of the $250 \times r$ sampled fields, we predict at the locations of the nodes

of the triangulation mesh conditionally on the sampled observations at the station locations. Thus, spatial predictions are compared with the simulated precipitation values in all mesh nodes. Figure 10 is RMSE, CRPS and coverage for the predictions averaged over all nodes, and for each r averaged over all replicates. The true model is non-stationary and both stationary and non-stationary models are fitted to the sampled datasets (observations at the 233 stations) and used for prediction. Figure 11 contains spatial plots of the pointwise difference in RMSE and CRPS. The non-stationary model does a better job predicting the non-stationary precipitation field. Averaged over nodes, the difference between the stationary and non-stationary models is relatively low. However, the difference is considerably larger in the mountain area in the middle of Norway. There are also other, but smaller, mountain areas where the difference is enhanced (cf. the elevation map in Figure 1b).

6 Discussion

In this paper, we have studied a non-stationary model with elevation as a spatial explanatory variable in the dependence structure. Furthermore, a framework for specifying prior distributions for the dependence structure parameters is suggested. Our proposed model was used for annual precipitation observations from southern Norway. We used five years of annual precipitation observations and assumed they came from independent realisations (replicates) of the underlying process. In addition to analysis of real precipitation data, we explored the spatial replicate model in a simulation study. The SPDE based model enables fast simulations and inference, which made it feasible to run simulations and evaluate statistical properties of the model when the number of replicates increases. The non-stationary model was compared to the corresponding stationary model in the simulations, and in the data analysis.

Key findings for the inference of parameters are that using replicates makes parameter estimates more precise and less prior sensitive, especially the dependence structure parameters θ_{NS} . These results are consistent for the case study and the simulation study. The simulation study also shows that having replicates improve statistical properties; the estimation bias is reduced and posterior credible interval coverage is improved when the number of replicates increases. The largest improvement is obtained changing from no replicates to two replicates. Also, using difference in DIC to choose between a stationary and non-stationary model gain power using replicates.

For the predictive performance, measured in average CRPS and RMSE, a slight improvement is achieved going from a stationary to a non-stationary model, but there are large local variations. Others have also reported only small improvements in predictive performance changing from a stationary to a non-stationary model (Paciorek and Schervish, 2006; Reich et al., 2011). Using replicates gives a slightly poorer predictive performance for the observation locations we have in our case

study. These results are consistent with the findings in the simulation study, where the coverage improved, but RMSE and CRPS increased with replicates.

We proposed a model with elevation both in the mean and covariance. The model was based on physical understanding of the precipitation process, and an attempt to handle the need to extrapolate with respect to elevation due to the placement of the rain gauges. In the simulation study, we were able to explore the differences in predictive performance on the entire domain, when stationary and non-stationary models were fitted to observations from a non-stationary model. We found that the largest differences in CRPS and RMSE were in mountain areas (Figure 11). Evaluation by cross-validation on the observation locations cannot give us this insight, neither for the case study nor for the simulation study, as there are no observations at high elevation.

The result in Figure 11 of course rely on the fact that the non-stationary replicate model we sample from is the true model. There are several signs that the model is, at least, reasonable: First, the difference in DIC between the stationary and non-stationary model is large (159), and agrees with what we expect from the simulation study (Figure 7b, with five replicates). Further, the posterior densities of parameters from individual models are similar, and posteriors of the parameters controlling the non-stationarity ($\theta_{\tau,h}$ and $\theta_{\kappa,h}$) are consistently shifted away from zero (Figure 4). This suggests that it is reasonable to model different years of annual precipitation as realisations of the same process, and that this process is non-stationary with elevation as an important explanatory variable.

More and other explanatory variables, in both the mean and covariance, will probably give us a better model. This has been outside the scope of the paper to investigate, but interesting explanatory variables to explore include other topographical explanatory variables and using aggregated output from reanalysis of weather models (Geirsson et al., 2014). The diversity of changes in local predictive performance between the models (Figure 3), illustrates the need for explanatory variables that capture the spatial variability, as well as good characteristics of local properties. Another important question is whether a non-stationary covariance is the best way to address spatial inhomogeneity. The measurement error is very likely to vary over the domain, and especially at wind exposed locations there is considerable measurement bias (Wolff et al., 2012). Fuglstad et al. (2014a) found that a simple model with a spatially varying nugget effect gave almost as good predictive results as a non-stationary model when they analysed annual precipitation in the conterminous US. To model the measurement error process more realistically, along with testing other explanatory variables, are natural paths to follow in the search for improved predictions and uncertainty estimates of precipitation in difficult and unmonitored terrain.

Ingebrigtsen et al. (2014) reported numerical problems, prior sensitivity and poor statistical properties. The proposed framework for specifying priors has given us a tool for setting priors for the dependence parameters controlling the non-stationarity. It is hard to have an intuition for these parameters. In addition, the parameters controlling the range ($\theta_{\kappa,1}$ and $\theta_{\kappa,h}$) are more challenging to identify

than the parameters controlling the marginal standard deviation ($\theta_{\tau,1}$ and $\theta_{\tau,h}$). Hence, the range parameters are more sensitive to the prior.

The variances of the non-stationarity parameters in Ingebrigtsen et al. (2014) corresponds to $c_\rho = 0.4$ and $c_\sigma = 0.6$, and 0.5- and 0.9-quantiles of the correlation range and marginal standard deviation are (154, 232) km and (0.282, 0.338) m. In comparison, these intervals were chosen to be (150, 500) km and (0.2, 2) m in this paper, and we used $c_\rho = 0.8$ and $c_\sigma = 1.3$, allowing for a higher relative change in nominal priors with respect to elevation. In this work, we did not experience numerical problems, and with the new priors there is less prior sensitivity, and bias and coverage are improved compared to Ingebrigtsen et al. (2014), also when using only one replicate.

The simulation study showed that if a non-stationary model is fitted to realisations sampled from a stationary model, both difference in DIC and posterior distributions of the non-stationarity parameters will indicate that the observations are from a stationary model. It is therefore little to lose by fitting a non-stationary model with explanatory variables that are thought to be of importance for the dependence structure. It is straightforward to change from a stationary model to a non-stationary model within the suggested SPDE modelling framework using the R-INLA software, and the inference is fast.

Fuglstad et al. (2014a) raise the question of whether non-stationarity is needed in spatial models. Their conclusion is yes, but that it is important to understand what type of non-stationarity the process exhibits. If there is knowledge about the driving forces of the physical process, explanatory variables in the dependence structure might be a fruitful way of modelling non-stationarity. Our analysis of the southern Norway data illustrates that priors for these type of models should be chosen with care, and that the dataset ideally should consist of more than one realisation of the process.

Acknowledgements

This work was supported by the project Spatio-temporal modelling and approximate Bayesian inference (196670/V30) funded by the Research Council of Norway.

References

- Banerjee, S., Carlin, B. P., and Gelfand, A. E. (2004). *Hierarchical Modeling and Analysis for Spatial Data*, volume 101 of *Monographs on Statistics and Applied Probability*. Chapman & Hall/CRC, Boca Raton, Florida.
- Bolin, D. and Lindgren, F. (2011). Spatial models generated by nested stochastic partial differential equations, with an application to global ozone mapping. *The Annals of Applied Statistics*, 5(1):523–550.

- Brenner, S. C. and Scott, L. R. (2007). *The Mathematical Theory of Finite Element Methods*, volume 15 of *Texts in Applied Mathematics*. Springer, New York, 3 edition.
- Cressie, N. and Wikle, C. K. (2011). *Statistics for spatio-temporal data*. Wiley series in probability and statistics. Wiley, Hoboken, New Jersey.
- Dyrrdal, A. V., Lenkoski, A., Thorarinsdottir, T. L., and Stordal, F. (2014). Bayesian hierarchical modeling of extreme hourly precipitation in Norway. *Environmetrics*. To appear.
- Fuentes, M. (2002). Spectral methods for nonstationary spatial processes. *Biometrika*, 89(1):197–210.
- Fuglstad, G.-A., Lindgren, F., Simpson, D., and Rue, H. (2014a). Do we need non-stationarity in spatial models? arXiv:1409.0743.
- Fuglstad, G.-A., Lindgren, F., Simpson, D., and Rue, H. (2014b). Exploring a new class of non-stationary spatial Gaussian random fields with varying local anisotropy. *Statistica Sinica*. To appear.
- Geirsson, Ó., Hrafnkelsson, B., and Simpson, D. (2014). Computationally efficient spatial modeling of annual maximum 24 hour precipitation. An application to data from Iceland. arXiv:1405.6947.
- Gelman, A. (2006). Prior distributions for variance parameters in hierarchical models (comment on article by Browne and Draper). *Bayesian Analysis*, 1(3):515–534.
- GLOBE Task Team (1999). Globe: The Global Land One-kilometer Base Elevation Digital Elevation Model, Version 1.0. <http://www.ngdc.noaa.gov/mgg/topo/globe.html>.
- Gneiting, T. and Raftery, A. E. (2007). Strictly proper scoring rules, prediction, and estimation. *Journal of the American Statistical Association*, 102(477):359–378.
- Hanks, E. M., Schliep, E. M., Hooten, M. B., and Hoeting, J. A. (2015). Restricted spatial regression in practice: geostatistical models, confounding, and robustness under model misspecification. *Environmetrics*. <http://dx.doi.org/10.1002/env.2331>.
- Higdon, D., Swall, J., and Kern, J. (1999). Non-stationary spatial modeling. In Bernardo, J. M., Berger, J. O., Dawid, A. P., and Smith, A. F. M., editors, *Bayesian Statistics 6. Proceedings of the Sixth Valencia International Meeting*, pages 761–768. Oxford University Press.
- Holand, A. M., Steinsland, I., Martino, S., and Jensen, H. (2013). Animal models and integrated nested Laplace approximations. *G3: Genes, Genomes, Genetics*, 3(8):1241–1251.

- Ingebrigtsen, R., Lindgren, F., and Steinsland, I. (2014). Spatial models with explanatory variables in the dependence structure. *Spatial Statistics*, 8:20–38.
- Kaufman, C. G. and Shaby, B. A. (2013). The role of the range parameter for estimation and prediction in geostatistics. *Biometrika*, 100(2):473–484.
- Lele, S. R., Nadeem, K., and Schmuland, B. (2010). Estimability and likelihood inference for Generalized Linear Mixed Models using data cloning. *Journal of the American Statistical Association*, 105(492):1617–1625.
- Lindgren, F. and Rue, H. (2014). Bayesian spatial modelling with R-INLA. *Journal of Statistical Software*. To appear.
- Lindgren, F., Rue, H., and Lindström, J. (2011). An explicit link between Gaussian fields and Gaussian Markov random fields: the stochastic partial differential equation approach (with discussion). *Journal of the Royal Statistical Society: Series B (Statistical Methodology)*, 73(4):423–498.
- NCAR - Research Applications Laboratory (2014). *verification: Weather Forecast Verification Utilities*. R package version 1.40.
- Neto, J. H. V., Schmidt, A. M., and Guttorp, P. (2014). Accounting for spatially varying directional effects in spatial covariance structures. *Journal of the Royal Statistical Society: Series C (Applied Statistics)*, 63(1):103–122.
- Orskaug, E., Scheel, I., Frigessi, A., Guttorp, P., Haugen, J. E., Tveito, O. E., and Haug, O. (2011). Evaluation of a dynamic downscaling of precipitation over the Norwegian mainland. *Tellus, Series A: Dynamic Meteorology and Oceanography*, 63A(4):746–756.
- Paciorek, C. J. and Schervish, M. J. (2006). Spatial modelling using a new class of nonstationary covariance functions. *Environmetrics*, 17:483–506.
- R Core Team (2013). *R: A Language and Environment for Statistical Computing*. R Foundation for Statistical Computing, Vienna, Austria. <http://www.R-project.org/>.
- Reich, B. J., Eidsvik, J., Guindani, M., Nail, A. J., and Schmidt, A. M. (2011). A class of covariate-dependent spatiotemporal covariance functions for the analysis of daily ozone concentration. *The Annals of Applied Statistics*, 5(4):2425–2447.
- Rue, H. and Held, L. (2005). *Gaussian Markov Random Fields: theory and applications*, volume 104 of *Monographs on Statistics and Applied Probability*. Chapman & Hall/CRC, Boca Raton, Florida.
- Rue, H., Martino, S., and Chopin, N. (2009). Approximate Bayesian inference for latent Gaussian models by using integrated nested Laplace approximations

- (with discussion). *Journal of the Royal Statistical Society: Series B (Statistical Methodology)*, 71(2):319–392.
- Sampson, P. D. and Guttorp, P. (1992). Nonparametric estimation of nonstationary spatial covariance structure. *Journal of the American Statistical Association*, 87(417):108–119.
- Schmidt, A. M., Guttorp, P., and O’Hagan, A. (2011). Considering covariates in the covariance structure of spatial processes. *Environmetrics*, 22:487–500.
- Simpson, D. P., Martins, T. G., Riebler, A., Fuglstad, G.-A., Rue, H., and Sørbye, S. H. (2014). Penalising model component complexity: A principled, practical approach to constructing priors. arXiv:1403.4630.
- Sørbye, S. H. and Rue, H. (2014). Scaling intrinsic Gaussian Markov random field priors in spatial modelling. *Spatial Statistics*, 8:39–51.
- Spiegelhalter, D. J., Best, N. G., Carlin, B. P., and Van Der Linde, A. (2002). Bayesian measures of model complexity and fit. *Journal of the Royal Statistical Society: Series B (Statistical Methodology)*, 64(4):583–639.
- Spiegelhalter, D. J., Best, N. G., Carlin, B. P., and Van Der Linde, A. (2014). The deviance information criterion: 12 years on. *Journal of the Royal Statistical Society: Series B (Statistical Methodology)*, 76(3):485–493.
- Whittle, P. (1954). On stationary processes in the plane. *Biometrika*, 41(3/4):434–449.
- Whittle, P. (1963). Stochastic processes in several dimensions. *Bulletin of the International Statistical Institute*, 40:974–994.
- Wolff, M., Isaksen, K., Brækkan, R., Alfnes, E., Petersen-Øverleir, A., and Ruud, E. (2012). Measurements of wind-induced loss of solid precipitation: description of a Norwegian field study. *Hydrology Research*.
- Zhang, H. (2004). Inconsistent estimation and asymptotically equal interpolations in model-based geostatistics. *Journal of the American Statistical Association*, 99(465):250–261.

Appendix A Figures

This appendix contains figures included for completeness of the results. [A.1](#) for the real annual precipitation dataset, and [A.2](#) and [A.3](#) for simulated datasets.

A.1 Southern Norway data

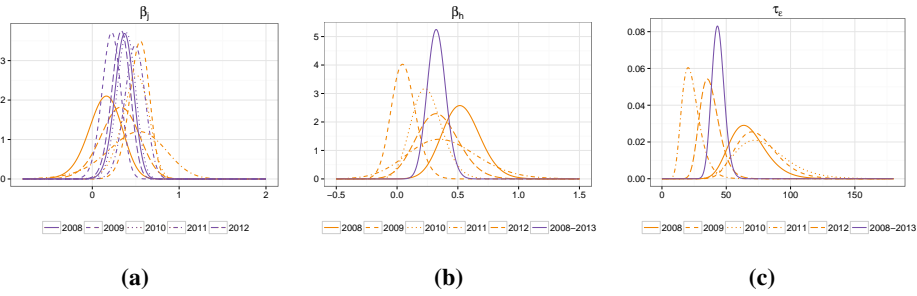


Figure 12: Posterior marginal densities for $\beta_j, j = 1, \dots, 5, \beta_h,$ and τ_ϵ with the non-stationary precipitation model. The individual model was fitted to each annual dataset and the replicate model was fitted to the five years together.

A.2 Simulation study: non-stationary datasets

This section contains results from the simulation study described in Section 5. It only includes results for the parameters $\beta_0, \beta_h,$ and $\tau_\epsilon,$ while results for the dependence structure parameters are in Section 5.2. The observations are sampled from the non-stationary model.

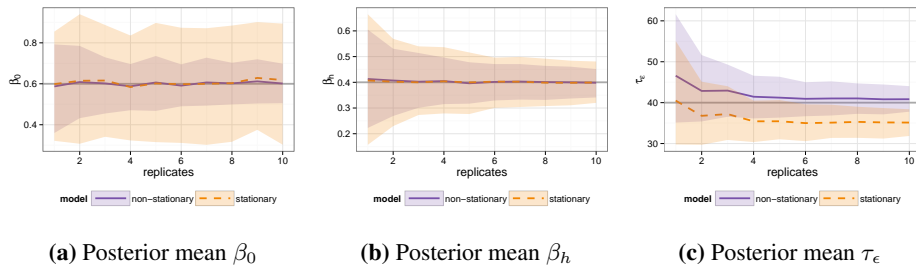


Figure 13: Stationary and non-stationary replicate models were fitted to datasets sampled from the non-stationary model. Presented are the posterior mean values for $\beta_0, \beta_h,$ and $\tau_\epsilon.$ The lines are averages over all datasets, while the shaded area span the range of the posterior mean values (between the 0.1- and 0.9-quantiles). The true parameter values are indicated with grey lines.

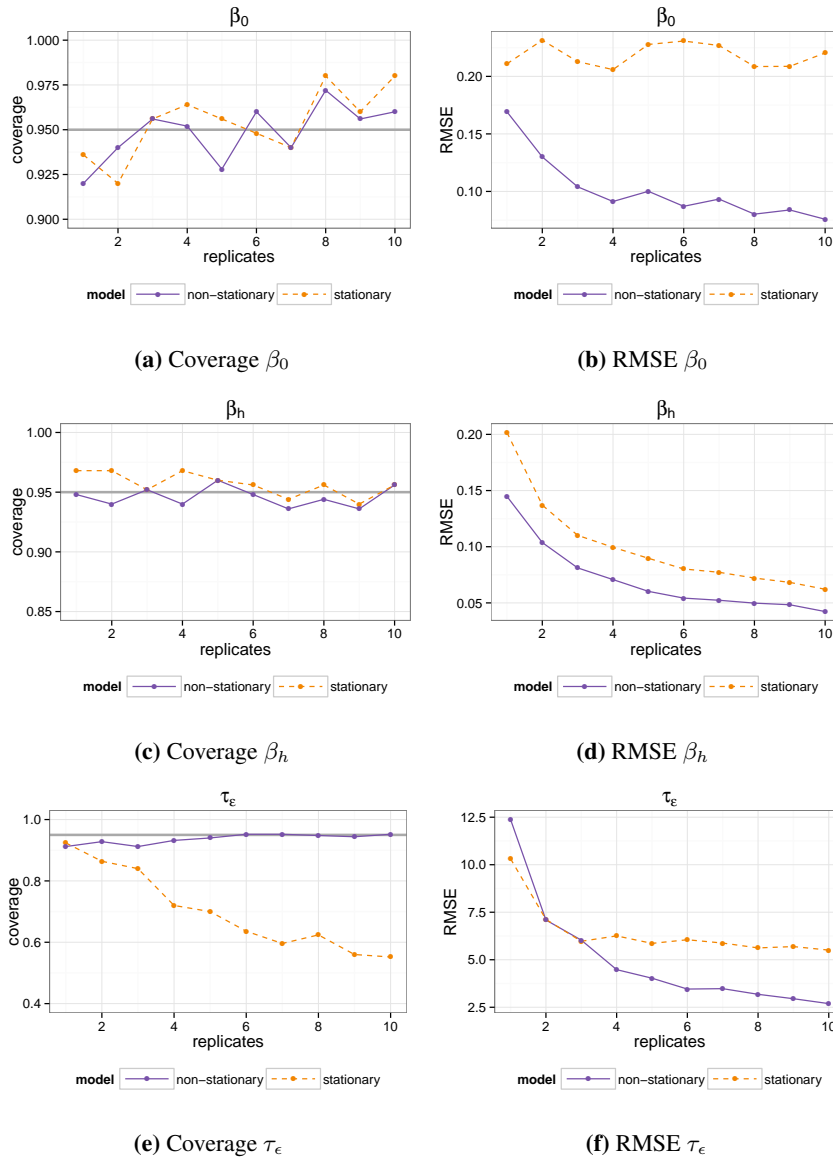


Figure 14: Stationary and non-stationary replicate models were fitted to datasets sampled from the non-stationary model. Presented are 95% posterior credible interval coverage and RMSE for the parameters β_0 , β_h , and τ_ϵ .

A.3 Simulation study: stationary datasets

This section contains results from the simulation study described in Section 5. Results for all model parameters are included, and the observations are sampled from a stationary model.

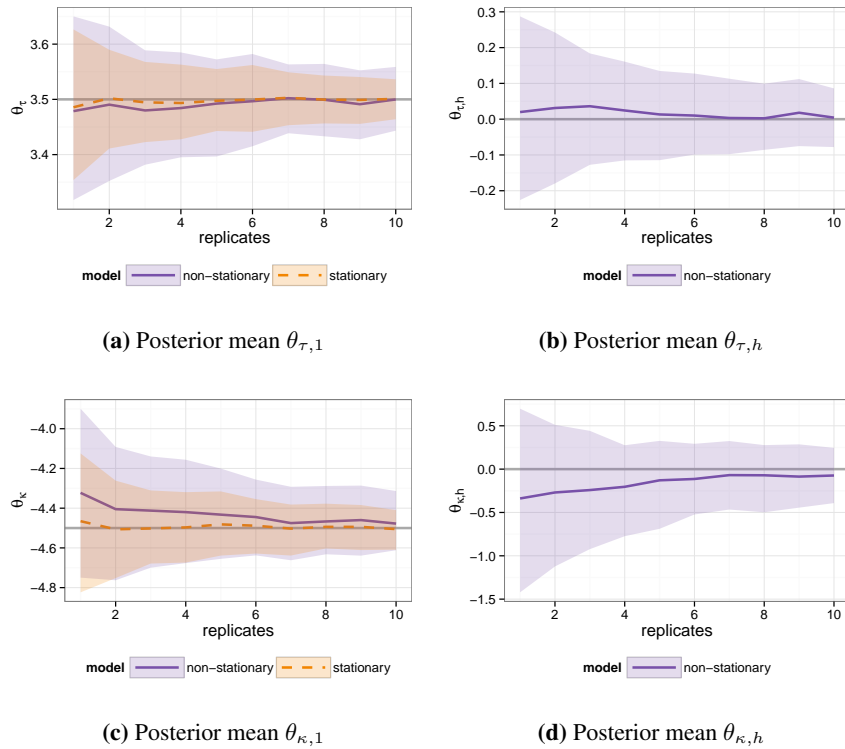


Figure 15: Stationary and non-stationary replicate models were fitted to datasets sampled from the stationary model. Presented are the posterior mean values for the spatial dependence structure parameters θ_S and θ_{NS} . The lines are averages over all datasets, while the shaded area span the range of the posterior mean values (between the 0.1- and 0.9-quantiles). The true parameter values are indicated with grey lines.

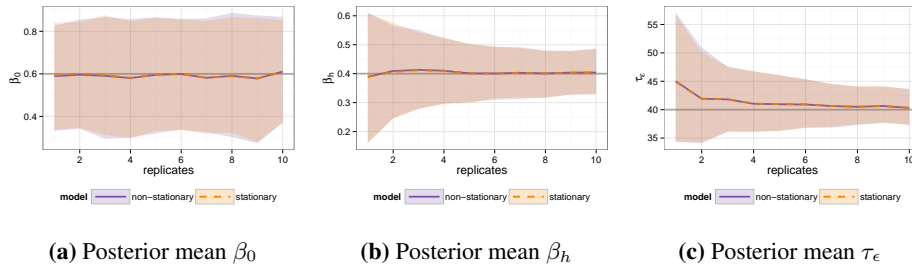


Figure 16: Stationary and non-stationary replicate models were fitted to datasets sampled from the stationary model. Presented are the posterior mean values for β_0 , β_h , and τ_ϵ . The lines are averages over all datasets, while the shaded area span the range of the posterior mean values (between the 0.1- and 0.9-quantiles). The true parameter values are indicated with grey lines.

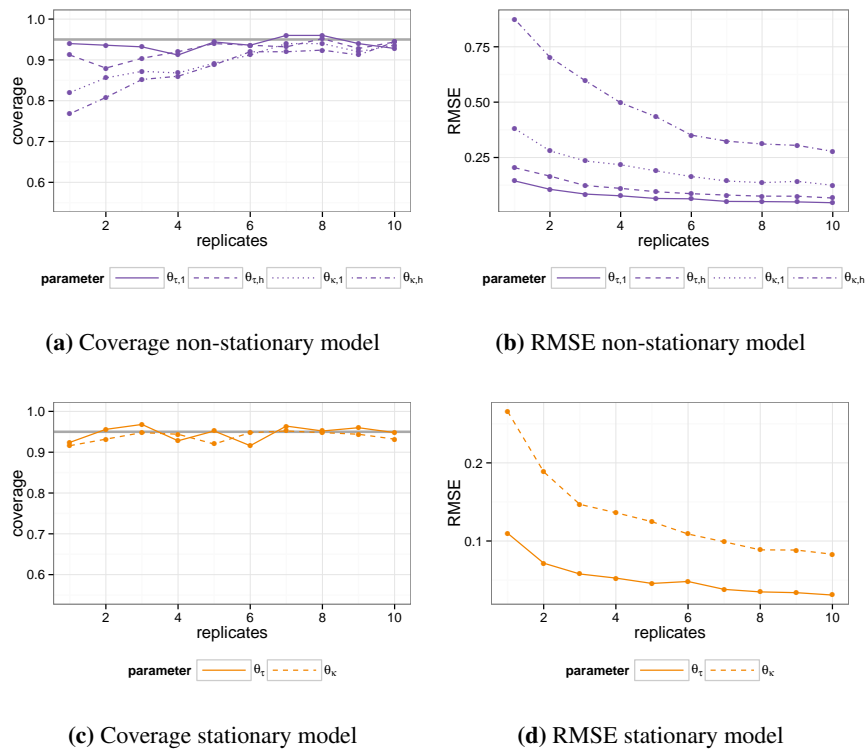


Figure 17: Stationary and non-stationary replicate models were fitted to datasets sampled from the stationary model. Presented are 95% posterior credible interval coverage and RMSE for the spatial dependence structure parameters θ_S and θ_{NS} .

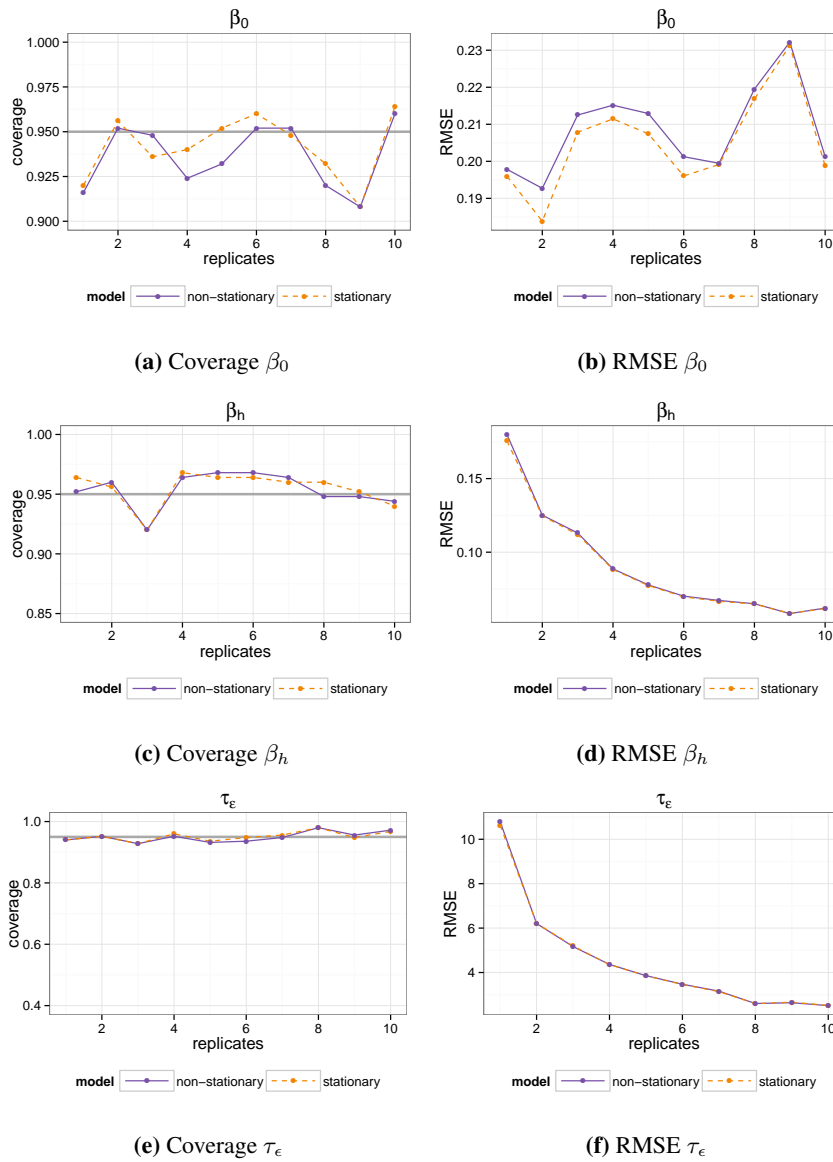


Figure 18: Stationary and non-stationary replicate models were fitted to datasets sampled from the stationary model. Presented are 95% posterior credible interval coverage and RMSE for the parameters β_0 , β_h , and τ_ϵ

Appendix B Prior sensitivity

In this appendix, the effect of using different coefficients of variation is investigated. The priors defined in Section 3.3 are used, but with different values for c_ρ and c_σ , thus different variances for the non-stationarity parameters $\theta_{\tau,h}$ and $\theta_{\kappa,h}$. The stationary priors (and non-stationary prior at sea level) are given by the 0.5- and 0.9-quantiles: 150 km and 500 km for the range, and 0.2 m and 2 m for the marginal standard deviation. This yields $\mu_\kappa = -3.97$, $\sigma_\kappa^2 = 0.88$, $\mu_\tau = 4.31$, and $\sigma_\tau^2 = 2.35$. The reference elevation h_0 is 0.4 km. Six different non-stationary priors are compared, these are summarised in Table 4. The prior labelled NS-2 is the one used in the paper. The prior labelled NS-1 is closest to the prior used in Ingebrigtsen et al. (2014). There, the prior means were set to $\mu_{\kappa,1} = -4$, $\mu_{\kappa,h} = 0$, $\mu_{\tau,1} = 4$, and $\mu_{\tau,h} = 0$, i.e. approximately the same as in this paper. The prior variances were set to $\sigma_{\kappa,1}^2 = 0.1$, $\sigma_{\kappa,h}^2 = 1$, $\sigma_{\tau,1}^2 = 0.1$ and $\sigma_{\tau,h}^2 = 1$, i.e. lower variances than what is used for the default prior in this paper.

Table 5 contains posterior quantiles for all model parameters for the replicate model and Table 6 for the individual model fitted to the 2008-2009 data. Cross-validated predictive scores are in Table 7. The results are stable with respect to choice of c_ρ and c_σ , most for the replicate model.

Table 4: Priors with different variances for the non-stationarity parameters $\theta_{\tau,h}$ and $\theta_{\kappa,h}$.

	NS-1	NS-2	NS-3	NS-4	NS-5	NS-6
c_ρ	0.4	0.8	1.6	0.8	0.8	3.5
c_σ	0.6	1.3	3.4	1.0	2.0	13
$\sigma_{\tau,h}^2$	0.99	3.09	7.88	1.24	6.97	15.95
$\sigma_{\kappa,h}^2$	0.93	3.09	7.94	3.09	3.09	16.15

Table 5: Posterior quantiles for the model parameters. The replicate model was fitted to the southern Norway 2008-2013 dataset, with stationary dependence structure (S) and non-stationary dependence structure (NS-). Six different priors were used for the non-stationary model.

parameter	quantiles	S	NS-1	NS-2	NS-3	NS-4	NS-5	NS-6
β_1	0.025	0.25	0.13	0.14	0.15	0.14	0.15	0.15
	0.500	0.70	0.35	0.37	0.37	0.36	0.37	0.37
	0.975	1.10	0.56	0.57	0.57	0.57	0.57	0.58
β_2	0.025	0.11	-0.01	0.00	0.00	-0.01	0.00	0.00
	0.500	0.55	0.21	0.22	0.22	0.21	0.22	0.22
	0.975	0.95	0.41	0.42	0.42	0.42	0.42	0.42
β_3	0.025	0.25	0.16	0.17	0.17	0.16	0.17	0.18
	0.500	0.70	0.38	0.39	0.40	0.39	0.40	0.40
	0.975	1.11	0.59	0.59	0.60	0.59	0.60	0.60
β_4	0.025	0.55	0.23	0.25	0.25	0.24	0.25	0.25
	0.500	1.03	0.47	0.49	0.49	0.48	0.49	0.50
	0.975	1.47	0.70	0.71	0.72	0.71	0.72	0.72
β_5	0.025	0.31	0.10	0.11	0.12	0.11	0.12	0.12
	0.500	0.75	0.32	0.33	0.34	0.33	0.34	0.34
	0.975	1.16	0.52	0.53	0.53	0.52	0.53	0.53
β_h	0.025	0.29	0.19	0.18	0.18	0.19	0.18	0.18
	0.500	0.49	0.33	0.32	0.32	0.33	0.32	0.32
	0.975	0.70	0.49	0.48	0.48	0.48	0.48	0.48
τ_ϵ	0.025	28.63	35.14	34.86	34.87	34.94	34.94	34.86
	0.500	35.45	43.62	43.51	43.29	43.42	43.39	43.33
	0.975	43.90	54.18	53.83	53.75	53.90	53.92	53.78
$\theta_{\tau,1}$	0.025	3.37	3.80	3.81	3.82	3.81	3.82	3.82
	0.500	3.49	3.94	3.96	3.96	3.95	3.96	3.97
	0.975	3.60	4.08	4.10	4.11	4.10	4.11	4.11
$\theta_{\tau,h}$	0.025		-1.55	-1.62	-1.65	-1.60	-1.63	-1.65
	0.500		-1.23	-1.29	-1.31	-1.27	-1.30	-1.31
	0.975		-0.93	-0.97	-0.98	-0.96	-0.97	-0.98
$\theta_{\kappa,1}$	0.025	-4.78	-6.16	-6.22	-6.24	-6.23	-6.22	-6.24
	0.500	-4.50	-5.84	-5.89	-5.91	-5.89	-5.89	-5.91
	0.975	-4.23	-5.53	-5.57	-5.58	-5.57	-5.57	-5.59
$\theta_{\kappa,h}$	0.025		2.66	2.75	2.77	2.74	2.75	2.78
	0.500		3.02	3.12	3.15	3.11	3.12	3.15
	0.975		3.39	3.51	3.54	3.50	3.51	3.55

Table 6: Quantiles of the posterior marginal distributions for all model parameters. The individual model was fitted to annual precipitation data from 2008-2009, with stationary dependence structure (S) and non-stationary dependence structure (NS-). Six different priors were used for the non-stationary model.

parameter	quantiles	S	NS-1	NS-2	NS-3	NS-4	NS-5	NS-6
β_1	0.025	0.02	-0.29	-0.26	-0.25	-0.28	-0.25	-0.24
	0.500	0.54	0.13	0.15	0.16	0.13	0.16	0.16
	0.975	0.96	0.48	0.49	0.50	0.48	0.50	0.50
β_h	0.025	0.35	0.26	0.24	0.23	0.25	0.23	0.23
	0.500	0.78	0.55	0.53	0.51	0.54	0.52	0.51
	0.975	1.22	0.88	0.85	0.84	0.87	0.85	0.84
τ_ϵ	0.025	32.21	43.35	43.60	43.62	43.54	43.67	43.58
	0.500	48.85	65.91	66.30	66.31	66.20	66.34	66.29
	0.975	73.61	99.69	99.96	99.99	99.83	100.08	99.95
$\theta_{\tau,1}$	0.025	3.28	3.63	3.67	3.68	3.66	3.67	3.69
	0.500	3.45	3.86	3.90	3.92	3.89	3.91	3.92
	0.975	3.64	4.09	4.14	4.16	4.12	4.15	4.16
$\theta_{\tau,h}$	0.025		-1.57	-1.73	-1.79	-1.68	-1.75	-1.81
	0.500		-1.09	-1.21	-1.25	-1.17	-1.22	-1.26
	0.975		-0.60	-0.70	-0.72	-0.67	-0.71	-0.73
$\theta_{\kappa,1}$	0.025	-5.19	-6.11	-6.30	-6.34	-6.30	-6.29	-6.36
	0.500	-4.61	-5.60	-5.74	-5.77	-5.74	-5.73	-5.79
	0.975	-4.11	-5.09	-5.20	-5.23	-5.20	-5.19	-5.24
$\theta_{\kappa,h}$	0.025		2.01	2.23	2.29	2.21	2.24	2.31
	0.500		2.61	2.85	2.92	2.83	2.86	2.95
	0.975		3.21	3.51	3.60	3.49	3.52	3.64

Table 7: Cross-validated predictive scores. The individual and replicate models were fitted to annual precipitation data from southern Norway, with stationary dependence structure (S) and non-stationary dependence structure (NS-). Six different priors were used for the non-stationary model.

	S	NS-1	NS-2	NS-3	NS-4	NS-5	NS-6
CRPS							
individual	0.1436	0.1383	0.1382	0.1383	0.1380	0.1383	0.1385
replicate	0.1438	0.1435	0.1436	0.1437	0.1435	0.1436	0.1437
RMSE							
individual	0.2655	0.2537	0.2531	0.2534	0.2530	0.2532	0.2536
replicate	0.2646	0.2565	0.2567	0.2569	0.2566	0.2568	0.2569